12-1-2020

# Petri Net modelling approach for analysing the behaviour of Wnt/[inline-formula removed] -catenin and Wnt/Ca 2+ signalling pathways in arrhythmogenic right ventricular cardiomyopathy.

Nazia Azim

Jamil Ahmad

Nadeem Iqbal

Amnah Siddiqa

Abdul Majid

*See next page for additional authors*

Authors
Nazia Azim, Jamil Ahmad, Nadeem Iqbal, Amnah Siddiqa, Abdul Majid, Javaria Ashraf, and Fazal Jalil

IET Systems Biology

*Research Article*

IET Journals
The Institution of Engineering and Technology

# Petri Net modelling approach for analysing the behaviour of *Wnt/β-catenin* and *Wnt/Ca*$^{2+}$ signalling pathways in arrhythmogenic right ventricular cardiomyopathy

ISSN 1751-8849
Received on 8th April 2020
Revised 20th June 2020
Accepted on 3rd August 2020
E-First on 23rd November 2020
doi: 10.1049/iet-syb.2020.0038
www.ietdl.org

*Nazia Azim[1], Jamil Ahmad[2] ✉, Nadeem Iqbal[1], Amnah Siddiqa[3], Abdul Majid[1], Javaria Ashraf[4], Fazal Jalil[5]*

[1]*Department of Computer Science, Abdul Wali Khan University Mardan, Mardan, Pakistan*
[2]*Department of Computer Science and Information Technology, University of Malakand, Chakdara, Pakistan*
[3]*Jackson Laboratory for Genomic Medicine, Farmington, Connecticut, USA*
[4]*Research Centre for modeling and Simulation, National University of Sciences and Technology, Islamabad Pakistan*
[5]*Department of Biotechnology, Abdul Wali Khan University Mardan, Mardan, Pakistan*
✉ *E-mail: jamil.ahmad@uom.edu.pk*

**Abstract:** Arrhythmogenic right ventricular cardiomyopathy (ARVC) is an inherited heart muscle disease that may result in arrhythmia, heart failure and sudden death. The hallmark pathological findings are progressive myocyte loss and fibro fatty replacement, with a predilection for the right ventricle. This study focuses on the adipose tissue formation in cardiomyocyte by considering the signal transduction pathways including *Wnt/β-catenin* and *Wnt/Ca*$^{2+}$ regulation system. These pathways are modelled and analysed using stochastic petri nets (SPN) in order to increase our comprehension of ARVC and in turn its treatment regimen. The *Wnt/β-catenin* model predicts that the dysregulation or absence of *Wnt* signalling, inhibition of dishevelled and elevation of glycogen synthase kinase 3 along with casein kinase I are key cytotoxic events resulting in apoptosis. Moreover, the *Wnt/Ca*$^{2+}$ SPN model demonstrates that the *Bcl2* gene inhibited by *c-Jun N-terminal kinase* protein in the event of endoplasmic reticulum stress due to action potential and increased amount of intracellular $Ca^{2+}$ which recovers the $Ca^{2+}$ homeostasis by phospholipase C, this event positively regulates the *Bcl2* to suppress the mitochondrial apoptosis which causes ARVC.

## 1 Introduction

Arrhythmogenic right ventricular cardiomyopathy (ARVC) is a heart muscle disease clinically characterised as life-threatening ventricular arrhythmias. Its prevalence has been estimated to vary from 1/2500 to 1/5000. ARVC is a major cause of sudden deaths in young people and specifically in athletes [1]. This disease is generally characterised by right ventricular (fibro)-fatty replacement of myocardial tissue with the clinical phenotype depicting cardiac arrhythmias, sudden cardiac death and heart failure [2].

Although being investigated from the past two decades, the molecular mechanisms of ARVC are sparsely spread across multiple research studies [3–6]. Despite there are several known disease-causing genes for ARVC, the molecular links among them have not been delineated. Lack of effective therapies in targeting the pathophysiology of ARVC further underpins the critical need to decipher its mechanistic basis [7]. Thus, there is a compelling need to develop refined disease models which could increase our understanding of the molecular mechanisms of pathogenesis of ARVC and allow prediction of experimental designs for testable hypotheses. Therefore, in this study, we aimed to develop and present the petri net-based models of two key signalling pathways (*Wnt/β-catenin* and *Wnt/Ca*$^{2+}$) which have been demonstrated to play a role in ARVC [3, 7, 8]. These models are based on our extensive literature survey effort conducted to first gather all molecular links in these signalling pathways which was then used to create biological regulatory networks (BRNs). The BRNs which encompass the regulatory feedback loops among key molecular entities in these signalling pathways were then transformed into respective petri net models (the employed methodologies have been comprehensively described in our previous work [9–12] and Section 2 below). These models were then used to simulate and predict the dynamical behaviour of the associated BRNs during homeostasis and pathological conditions that may underpin ARVC. The predicted results of these models are inline with the previous experimental observations and thus may have potential therapeutic implications for treatment of ARVC. To the best of our knowledge, this is a very first attempt to present an ARVC-based molecular disease model based on petri net approach which will open avenues for further experimental research in target identification and may aid in therapeutic interventions.

The molecular pathogenesis of ARVC has at least two components including fibroadiposis and cardiac dysfunction. Two different arms of intracellular signalling of the *Wnt* pathway are (i) the *Wnt/β-catenin* pathway and (ii) the *Wnt/Ca*$^{2+}$ pathway [13], both have been demonstrated to be deregulated in ARVC and described comprehensively below.

### 1.1 Signalling pathways

The gating mechanisms of mechanosensitive cardiomyocytes are used to modulate the cardiomyocyte responses to genetic abnormalities and stress of the system. The basis for the mechano-transduction system is formed by the network of complex proteins through which extracellular matrix (ECM) and sarcomere are connected with each other. For example, the intracellular signalling and sarcomere connection with ECM by integrins are performed via components of complex costamere, which alter the regulation of transcription in response to distortion of membrane and properties of contraction. In response to systemic stress, the signal is initiated which is implemented by mechanosensitive channels of ions. The signalling pathways are induced by changes in stress of cardiomyocyte which is connected with progression of cardiac pathology [14].

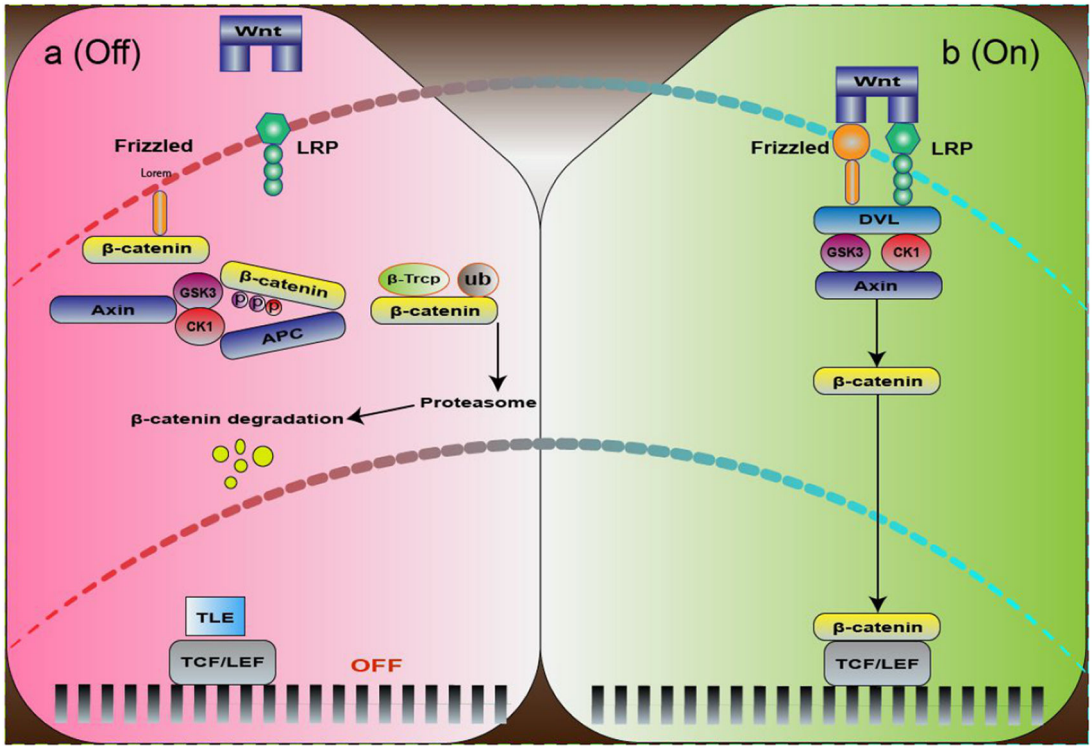


**Fig. 1** *Physiological and pathophysiological signaling of Wnt- β-catenin pathway*

***(a)*** In the absence of Wnt ligand *β*-catenin is degraded which gives rise to pathophysiological phenotypes, ***(b)*** When Wnt ligand is present then *β*-catenin will translocate to nucleus and activates Wnt responsive genes and maintain homeostasis

The important mechanisms of cardiomyocytes such as cell generation, polarity of the cell, homeostasis of tissues and fate of cell during the development of embryo are initiated by the *Wnt* ligand (secreted glycolipoproteins) [13]. The absence of *Wnt* disturbs the *Wnt* pathway which can cause defects in human birth, cancer etc. In heart tissue, homeostasis of *Wnt/β-catenin* pathway plays an important role in adults. Dysregulation of this signalling pathway causes many cardiac pathological conditions such as hypertrophic cardiomyopathy, myocardial infarction, ARVC.*Wnt/β-catenin* is the molecular disease of ARVC in which substitution of the adipose tissue occurs in the myocardium [15].

The schematic diagram of *Wnt/β-catenin* signalling is illustrated in (Fig. 1). The *β-catenin* in the cytoplasm is degraded continuously by *Axin* complex in the absence of *Wnt* ligand. The Axin complex is composed of *Axin* protein, adenomatous polyposis coli *(APC)*, glycogen synthase kinase 3 *(GSK3)* and casein kinase I *(CKI)*. *β*-transducin repeats-containing proteins *(β-TrCP)* identifies and degrades *β-catenin* after the sequential phosphorylation of *β-catenin* by *CK1* and *GSK3*. This will prevent *β-catenin* translocation to the nucleus which will eventually represses the activation of *Wnt* target genes by Factor/T-cell-specific transcription factor *(Tcf/Lef)* (Fig. 1*a*). On the other hand in the presence of *Wnt*, the *β-catenin* pathway is initiated (Fig. 1*b*). Here, *Wnt* binds with *Frizzled* and its co-receptor Factor/T-cell-specific transcription factor *(LRP5/6)*. The former is a seven-pass transmembrane protein receptor while its co-receptor is low-density lipoprotein. The complex of *Wnt-Frizzled* (*Wnt/Frizz*) activates dishevelled *(Dvl)* and *Axin* leading to inhibition of *β*-catenin phosphorylation. It prevents *β-catenin* degradation which then translocates to the nucleus and makes a complex with *Tcf/lef* activating downstream *Wnt* responsive genes (Fig. 1*b*) [16].

The *Wnt* ligand binds to *FRIZZLED (Frizz)* receptor which further activates many intracellular molecules and signalling pathways, i.e. diglyceride (*DAG*), Inositol 1,4,5-trisphosphate *(IP3)* and $Ca^{2+}$ (Fig. 2). The increase of these messengers affects the functions of the cell. The phospholipase C *(PLC)* activates the *IP3* and DAG are derived from membrane-bound *phospholipid phosphatidyl inositol 4, 5-bisphosphate*. The *Wnt* and *Frizz* interaction activates the *PLC*. The *IP3* moves into the cytosol and releases extra $Ca^{2+}$ ions stored and present in the endoplasmic reticulum (ER) membrane [17].

$Ca^{2+}$ is a second messenger in the cell which is involved in different processes of signalling such as cardiac contraction, hormones secretion, neurotransmission and growth factor etc. $Ca^{2+}$ influx and efflux into the cell are carried out by voltage-gated channels (VGCs), energy-dependent apparatuses as well as by receptor-based signalling. Together they maintain homeostasis in the cell but cellular perturbations such as stress response in ER in the initial and late stage of apoptosis disrupt homeostasis and signalling of $Ca^{2+}$. $Ca^{2+}$ plays a major role in cell death and its overload induce apoptosis [18]. $Ca^{2+}$ influx into the plasma membrane activates many basic functions of the cell and the reloading of $Ca^{2+}$ in ER after depletion of $Ca^{2+}$ from the ER store. The ER $Ca^{2+}$ ions release and activate the $Ca^{2+}$ influx to the ER store [19].

When unfolded proteins aggregate in ER, *Binding-immunoglobulin protein* separates from the complex of *inositol-requiring protein-1 (IRE1), Protein kinase RNA-like ER kinase (PERK)* and *Activating Transcription Factor-6 (ATF6)* in turn activating them. *IRE1* then recruits *tumour necrosis factor receptor-associated Factor-2 (TRAF2)* and *apoptosis-signalling-kinase 1*, which then results in downstream activation of *c-Jun N-terminal protein kinase (JNK)* and *p38 mitogen-activation protein kinase (MAPK)*. The CCAAT enhancer-binding protein homologous protein *(CHOP)* is activated by *p38 MAPK* phosphorylation while, *JNK* translocates to the mitochondrial membrane, where it inhibits *Bcl2*. The *Bcl2-associated X (Bax) protein* and *Bcl2 homologous antagonist killer (Bak) protein* are activated by IRE1 which induce *inositol 1, 4, 5-triphosphate receptors (IP3Rs)* and causes $Ca^{2+}$ release from the ER [18].

The influx of extracellular $Ca^{2+}$ ions into the cell occurs through $Ca^{2+}$ VGCs and many ligand-gated channels (LGCs) due to action potential. Translocation of $Ca^{2+}$ ions from ER into cytoplasm occurs through *Ryanodine Receptors (RyRs)* or *IP3Rs*. Increase in the level of intracellular $Ca^{2+}$ ions due to ER stress response causes depolarisation of the memebrane. The activation of *Bak* and *Bax* in the membrane of ER allows the $Ca^{2+}$ release into the cytosol where it activates the *m-Calpain* and finally activates

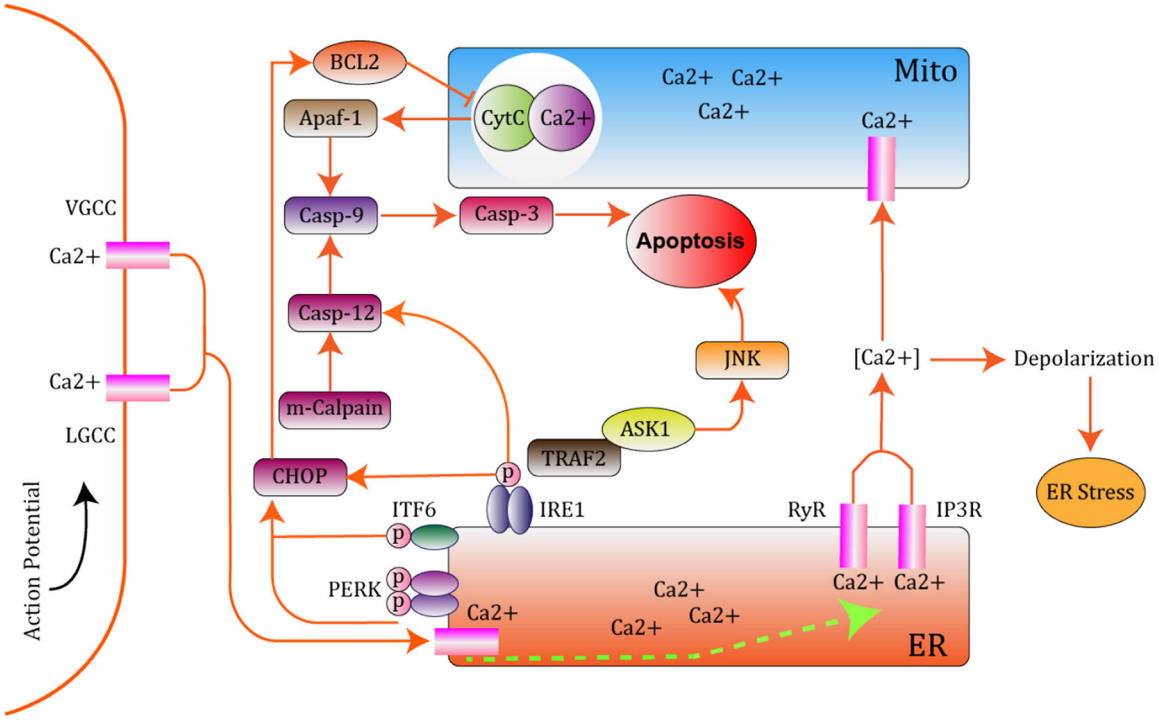


**Fig. 2** *Physiological role of* $Ca^{2+}$ *channel during the initiation of action potential. The imbalance of* $Ca^{2+}$ *homeostasis causes apoptosis which results in ARVC*

the *procaspase-12* which lead to the activation of the caspase cascade. $Ca^{2+}$ also move to mitochondria, which lead to the membrane depolarisation and releases *cytochrome c* and apoptotic protease activating factor 1/procaspase-9-regulated is activated to cause apoptosis. The *PERK* and *ATF6* trigger *CHOP* that is pro-apoptotic at downstream. The *IRE1* is also activated by ER stress which further leads to activation of *ASK, TRAF, JNK* and *procaspase-12* which finally trigger caspase cascade [18].

The regulation of cytoplasmic $Ca^{2+}$ is carried out at low level as compared to extracellular $Ca^{2+}$ through homeostatic mechanism created by voltage and receptor-operated channels. These mechanisms are used to maintain equilibrium between $Ca^{2+}$ inside the cell and $Ca^{2+}$ to extracellular space [20]. The $Ca^{2+}$ efflux is carried out by plasma membrane calcium ATPase (PMCA) channel and sodium–calcium exchanger (NCX) which are ATP dependent membrane pumps. Many physiological processes use proteins activated by high $Ca^{2+}$ inclusion in the cell. One of the influx channels is the N-methyl-D-aspartate receptor, which maintains $Ca^{2+}$ influx when it binds to ligand (glu) to get switched ON. Another type of $Ca^{2+}$ influx gateway is the voltage-gated $Ca^{2+}$ channel (VGCC). The VGCC gets switched ON to depolarise the plasma membrane because of $Ca^{2+}/Na^{+}$ ions exchange [21, 22]. The store-operated channels increase $Ca^{2+}$ ions influx into ER $Ca^{2+}$ from the cytoplasm. The Ryanodine (RyRs) and IP3 sensitive pathways are responsible for the calcium exchange in ER. The G-protein coupled receptor (GPCR) activates PLC which release $Ca^{2+}$ by IP3. The extracellular $Ca^{2+}$ concentration is managed by NCX and PMCA channels [20].

### *1.2 Contribution*

The study was conducted to provide a clear understanding of the role of *Wnt/β-catenin* and *Wnt/*$Ca^{2+}$ in the progression of ARVC by investigating the underlying dynamics of associated molecular entities. The main contribution of this study is the construction of stochastic petri net (SPN) models of *Wnt/β-catenin* and *Wnt/*$Ca^{2+}$ pathways which provide comprehensive insights into the possible signalling dynamics of associated BRNs during homeostasis and pathophysiological conditions. The dynamics of pathophysiological behaviours of cardiomyocyte analysed through these models could predict dynamics under different scenarios e.g. How the absence of *Wnt* ligand disrupt the Wnt signalling pathway to cause apoptosis? How the activators (*PP1* and *PP2A* etc.) and inhibitors (*GSK, Axin, BCl2* etc) regulate the *Wnt* signalling and calcium pathways through positive and negative regulatory feedback loops. The model demonstrates molecular dynamics in the absence of *Wnt* signalling where inactivation of *Dvl* causes the *GSK3* to inhibit the translocation of *β-catenin* to the nucleus and in turn leading the cellular apoptosis. Overall, the results demonstrate an intertwined dysregulation of molecular entities in *Wnt* signalling, *β-catenin* degradation and imbalance of calcium signalling homeostasis which upon further investigation warrants the therapeutic implications. Moreover, the predicted results are in agreement with those observed in previous experiments (see Section 3).

## 2 Methodology

The methodological steps followed in this study to model the biological signalling pathways *Wnt/β-catenin* and *Wnt/*$Ca^{2+}$ of ARVC is graphically illustrated in Fig. 3 and explained in-depth in the following sections.

### *2.1 Petri net modelling*

Petri net is a very dynamic mathematical formalism for modelling of real systems initially utilised for the biochemical systems in 1939 [21]. After that many biological systems have been modelled using petri net approach on the basis of its simplicity and flexibility (some recent examples are [10, 12, 23–25]). These models facilitate us to present the dynamic behaviour of time-dependent systems. A mathematical platform as provided by petri nets to analyse and test the hypothesis of biologists for experiments is now well established [26–28].

A petri net is a bipartite graph comprising of two types of nodes, i.e. places (represented by circles) and transitions (represented by square/rectangle) [29]. The biological entities, e.g. gene, protein, mRNA, ions and other cellular components are represented by places (◯) while the biochemical reactions, e.g. activation, inhibition, dephosphorylating, phosphorylation and translocation are represented by transitions (□) [20]. A directed arc connects a place with a transition. Real numbers or discrete integers (also called tokens) in the places models the quantities of the molecular entities they are representing. The flow of these

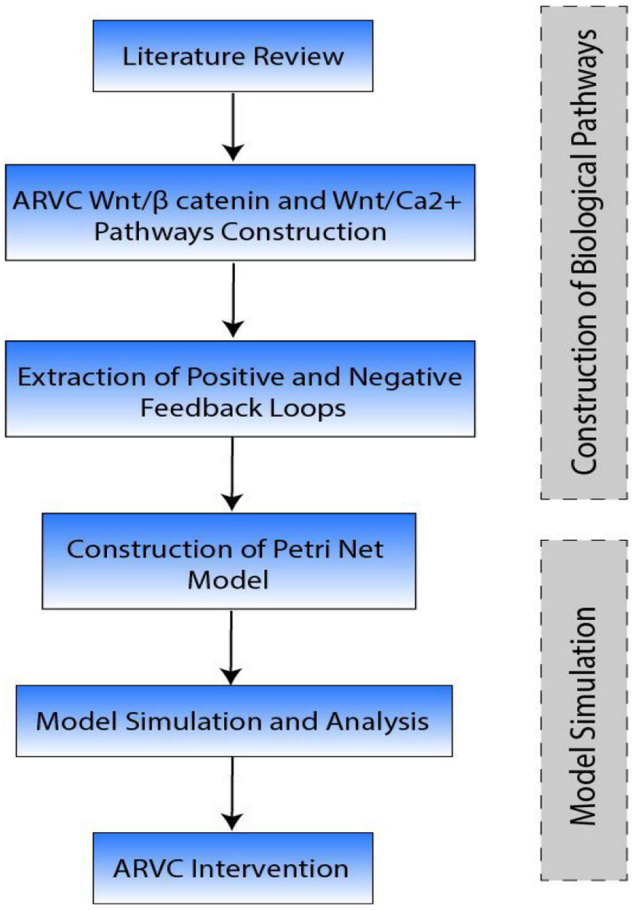


**Fig. 3** *Modelling and analysis workflow. The steps followed in methodology are illustrated*

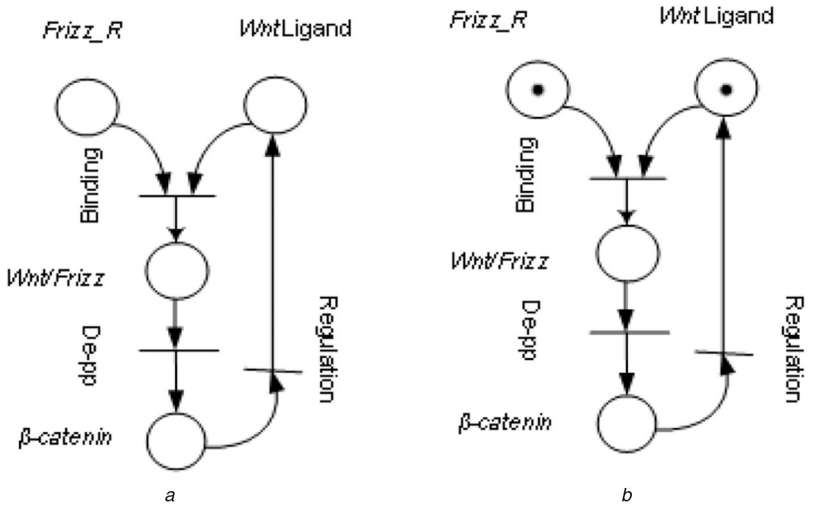


**Fig. 4** *Unmarked petri net model of Wnt signalling pathway*
***(a)*** Wnt/Frizz complex is formed by binding transition. The place $\beta$-catenin is dephosphorylated by De-pptransition which regulates Wnt ligand in a positive feed back loop by $\beta$-catenin at regulation transition, ***(b)*** Marked petri net model has tokens which represent initial marking of the Wnt signalling model

quantities between places (pre and post) takes place through a process called the firing of transitions. An enabled transition (having sufficient tokens equivalent to or greater than a multiplicity of the arc weights) may fire modelling the flow of quantities from pre-places to post-places. At a time instant $t$, the markings of all places of a petri net specify its state. Formal semantics of petri nets given below have been adopted from Ashraf *et al*. [20]. However, readers are directed to several recent studies for more insights into the application and usage of petri nets in modelling biological systems [29–31].

*Definition 1: (Unmarked petri net*). There are five components in unmarked petri net $P = < \rho, \tau$ and $\varepsilon$, pre, post>. Where

- $\rho$ consists of a finite set of places, i.e. $\rho = \{\rho_1, \rho_2, \rho_3, \ldots, \rho_n\}$.
- $\tau$ consists of a finite set of transitions, i.e. $\tau = \{\tau_1, \tau_2, \tau_3, \ldots, \tau_n\}$.
- $\rho \cap \tau = \phi$, both $\rho$ and $\tau$ cannot be empty sets.
- $\varepsilon \subseteq \rho \times \tau \cup \tau \times \rho$ consists of transitions' edges (input and output).
- Pre: $\rho \times \tau \rightarrow N$, non-negative values assigned by a weight function to an input edge.
- Post: $\tau \times \rho \rightarrow N$, non-negative values assigned by a weight function to an output edge.

An unmarked petri net is shown in Fig. 4*a*, for modelling of *Wnt* signalling pathway. The places *Frizz_R* and *Wnt* ligand form a

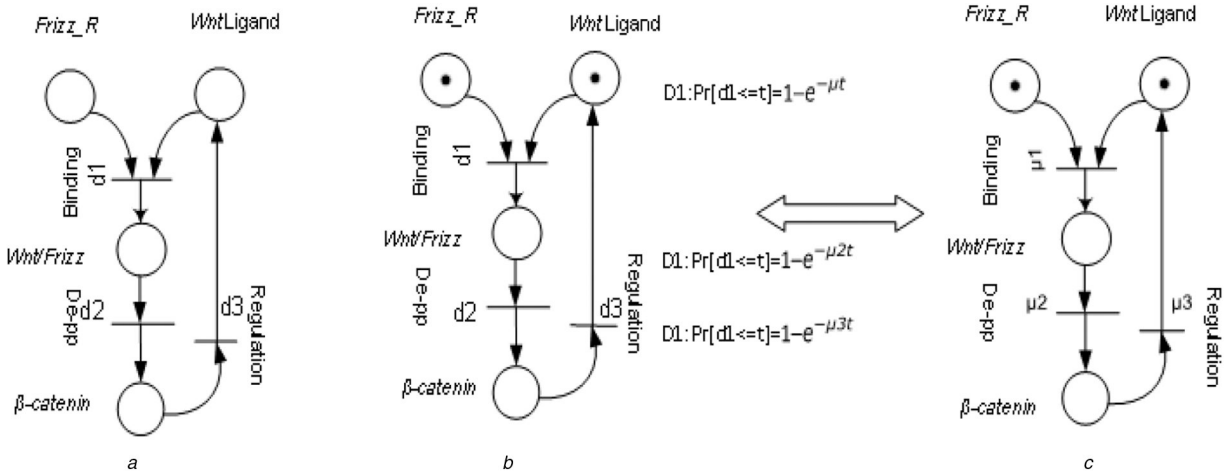


**Fig. 5** *Wnt signalling pathway using TPN model*

***(a)*** The Wnt and Frizz components bind to make a complex Wnt/Frizz. The transitions binding, De-pp and regulation are associated with time delay $d1$, $d2$ and $d3$, respectively. The transitions are fired when the associated time delay ($d1$, $d2$ and $d3$) is elapsed, ***(b), (c)*** Shows specified and usual SPNs. The TPN can be converted into SPN when the deterministic firing function d changes into a random variable

complex *Wnt/Frizz* which further activates the *Wnt* signalling pathway.

*Definition 2:* (*Marked petri net*). The marked petri net (MPN) consist of MP = < $P$, m $\breve{0}$ > where

- $P$ =< $\rho, \tau, \epsilon$, pre, post> is an unmarked petri net and
- $m\ \breve{0}$: $\rho \rightarrow Z_{\geq 0}$ is the petri net initial marking.

*Definition 3:* [*Timed petri net (TPN)*]. The TPN have TP = < MP, $\breve{f}n$ > where

- MP =< $P$, $\breve{m}$ >> is an MPN.
- $\breve{f}n$: $\tau \rightarrow \mathrm{R}^+$ is a function that assigns a positive real number, i.e. each transition's a time delay.

A TPN has $d_i$ time delay associated with transition $\tau_i$. When the Pre place has sufficient tokens then transition gets enabled and fired its specific time delay elapsed as shown in Fig. 5*a*. When the variables of time delays are random then SPN is used. SPN is derived from TPN presented in Fig. *c* [10].

*Definition 4:* (*SPN*). An SPN is a marked petri net which is pair of MP, Rate where MP = $(P, \breve{m}_0)$ is a MPN (marked petri net) and Rate: $\tau \rightarrow R^+$, which is a function from the transition set $\tau$ to the positive finite real numbers set. Rate $(\tau_i) = \mu_i$, is the transition firing rate of transitions $\tau_i$. In equation (1)$d_i$ have been assigned random variables of negative exponential for probability distribution function $\breve{f}n(t)$,

$$\breve{f}n(t) = Pr[d_i \leq t] = 1 - \mathrm{e}^{-\mu_i t} \tag{1}$$

where, $Pr[d_i \leq t + dt | d_i > t] = \mu_i \cdot \mathrm{d}t$

The firing frequency of transitions and their time-dependent flow of tokens are simulated over multiple runs to get an average in SPNs [28]. In order to reproduce the time-dependent dynamic behaviour of the biological system under study, the firing rates can be determined either experimentally or inferred by trial and error [28]. SPN has its underlying semantics of discrete-time Markov chain and mainly all algorithms for stochastic modelling of biochemical processes are based on the Gillespie's algorithm described in [32]. Moreover, the snoopy tool also uses Gillespie's algorithm for stochastic modelling of petri nets [33–35]. An SPN is especially suitable for modelling of bio-molecular networks [29]. Several studies have comprehensively described in sufficient details the inherent stochasticity of different bio-molecular systems including gene regulation, signalling pathways and other biochemical reactions and we refer our readers to them for more insights [23, 36].

The SNOOPY tool [37] has been used to design, stimulate and animate the biological network of signalling pathways previously and in this study as well [22]. The discrete steps involved in petri net modelling in this study includes the abstraction of extracted pathway iteratively; find out the pathway positive and negative feedback loops to regulate the signalling pathway against ARVC; petri net model construction, analysis and model verification through simulation Fig. 3.

## 3 Results

In this study, the biological signalling networks of *Wnt/β-catenin* and *Wnt*/$Ca^{2+}$ pathways for ARVC disease are constructed as shown in Fig. 6 and 7, respectively. Three SPNs were then constructed which are presented in Figs. 8–10, respectively.

### *3.1 Construction of the Wnt/β-catenin and Wnt/*$Ca^{2+}$ *ARVC pathway*

The biological pathways for *Wnt/β-catenin* and *Wnt*/$Ca^{2+}$ signalling networks are constructed from a detailed study of literature review and are presented in Figs. 6 and 7, respectively. The deregulation in *Wnt* signal and $Ca^{2+}$ concentration level cause the phenotype of ARVC. Fig. 6 shows the absence of *Wnt* signal causes the high level of *GSK3* and *Ck1* which negatively regulates the pathways and degrades the *β-catenin* and hence results in adipose tissues formation and heart failure. There are several positive and negative feedback loops present in the pathway which regulates it. Fig. 7 depicts that the action potential increases cytosolic $Ca^{2+}$ levels. This in turn creates the ER stress triggering apoptotic pathways via mcalpin in the cytoplasm. On the other hand, $Ca^{2+}$ overload in mitochondria raptures the membrane of mitochondria and release the cytochrome C in the cytoplasm to activate the caspase cascades which also stimulate apoptosis. The ER and $Ca^{2+}$ in cytoplasm activate the *IRE1* which proceed to activate the pro-apoptoic component *JNK*, which inhibit the anti-apoptotic gene *Bcl2*. The *Bak* and *Bax* are pro-apoptotic components which can be inhibited by *Bcl2*. The ER stress activates CHOP which inhibits *Bcl2*.

### *3.2 Modelling approach for ARVC pathway*

Based on the BRNs shown in Figs. 6 and 7, three SPNs were constructed which are presented in Figs. 8–10, respectively. Single SPN was constructed to model both cases of homeostasis and pathogenesis for Wnt/*β*-catenin signalling pathway (Fig. 8). Whereas two different SPNs were constructed to model

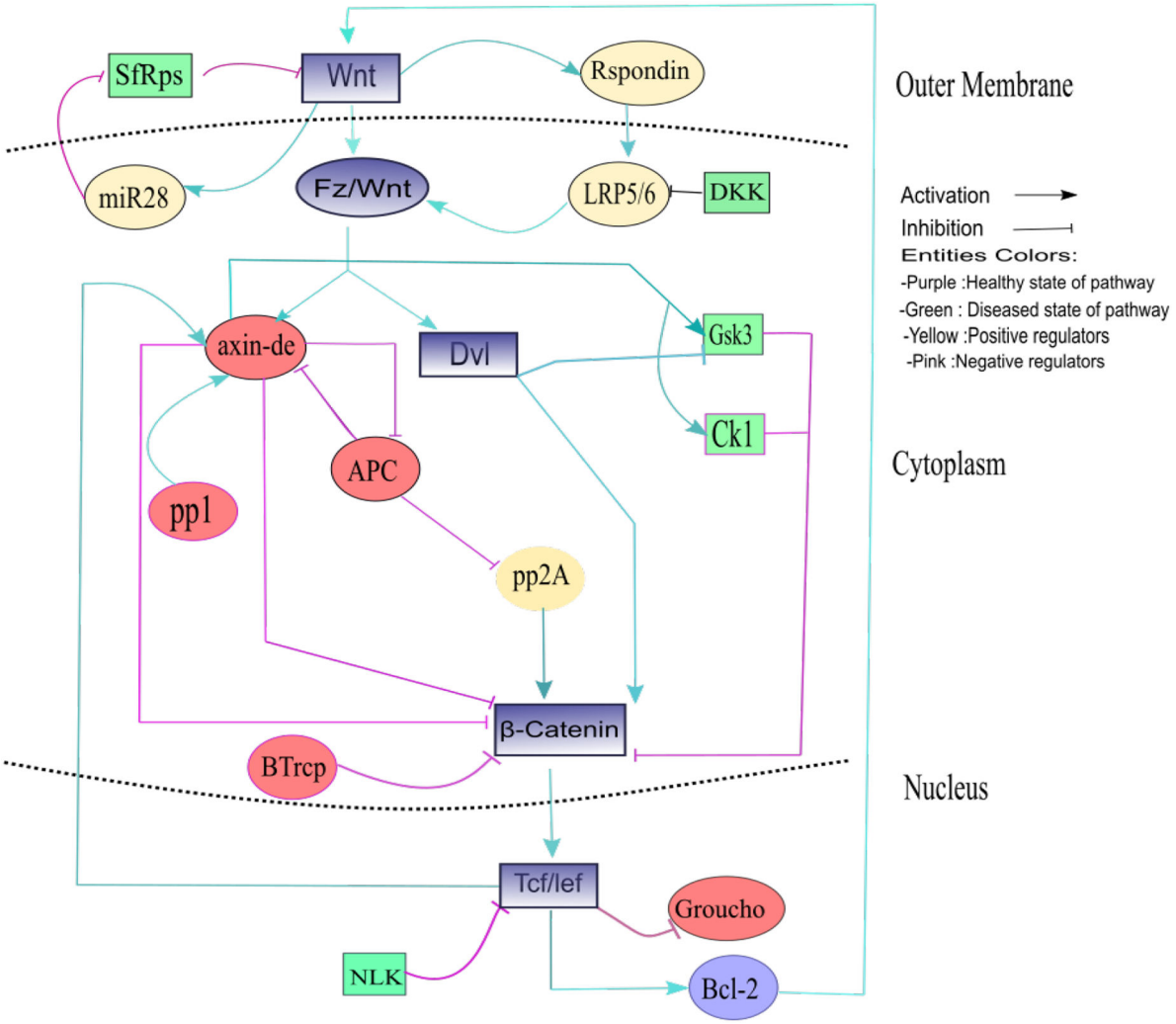


**Fig. 6** *Wnt/β-catenin signalling pathway shows positive regulation through a positive feedback loop among Wnt, Dvl, β-catenin, Tcf/lef and Bcl2. While GSK3 and Ck1 negatively regulates β-catenin in the pathway*

homeostasis and pathogenesis scenarios for *Wnt*/$Ca^{2+}$ signalling pathway(Figs. 9 and 10, respectively). Usually, different sets of parameters are sufficient to model different scenarios when modelling a petri net because of the same underlying molecular interactions with different rates which was the case for Wnt/*β*-catenin pathway. However, we had to construct two SPNs for *Wnt*/$Ca^{2+}$ signalling pathway in order to model and display the additional molecular events initiated in case of its deregulation. Software tool SNOOPY (version 2.0.33 for windows) was used to generate and simulate the model. Every simulation was performed 1000 times. The parameters were generated to visualise the homeostatic and stable state behaviours in these models by trial and error and matched with experimental observations for validation (Table 1 and 2). These parameters calculate the random time delay variables for the time of activation and inhibition. The petri net model exported in SBML format using Snoopy tool are provided as Supplementary Files (1–3).

*3.2.1 SPN model of* ***Wnt****/β-catenin signalling:* The biological model of *Wnt/β-catenin* in Fig. 6 is converted into SPN model which is presented in Fig. 8. In the modelled petri net there are many activators and inhibitors that are regulating the dynamics. The transition rates of homeostatic and ARVC pathological phenotype are given in Tables 3 and 4, respectively. In order to model the pathology in the pathway, the rate of the mass actions is tuned in accordance with experimental data cited in Table 1. In SPN model initially, due to the inhibitor at place *secreted frizzled-related proteins (sFRPs)*, the *Wnt* ligand is suppressed and *Wnt* signalling pathway is dysregulated as shown in Fig. 6. The transitions of the system are labelled with 't'. The transition t1 inhibits *Wnt* ligand when *sFRPs* token is present to lower the *Wnt* level and the t2 transition suppresses the place *sFRPs* by place *miR28* at a high rate in Table 3, shown in Fig. 11*a*. The *Wnt* ligand positively regulates the *miR28* using the transition t3.

Table 3 shows the transition rates of homeostatic state of the pathway where the high value of transitions shows that these components recover the pathway from disease by decreasing transition values of inhibitors at low transition rates in the table. The transition t4 activates place Rspondin which regulates the receptor at place LRP5/6 by t5, respectively, represented in Fig. 11*b*. Through transition t6 at a high rate in Table 4 the place marked by *Dickkopf (DKK)* inhibits the receptor LRP5/6 to inhibit the binding of places *Wnt* and *Frizz* receptor in Fig. 12*b*. In the absence of *Wnt* ligand, the *Frizz* receptor does not bind with it to make a complex of place *Wnt/Frizz* to further activate the *Wnt* pathway. The *Wnt* ligand and *Frizz* receptor with its co-receptor LRP5/6 make a *WLF* complex at high transition rate t7 in Table 3 and shown in Fig. 12*a*. The transition t9 shows that *WLFComplex*, *Dvl* and *axin* makes a new complex *WLFA*.

The *Wnt/Frizz* complex will further activate the place *Dvl* and dephosphorylates *β-catenin* as shown in Fig. 13*a* by transition t8. The *Dvl* further leads to inhibit the place *GSK3* and degradation of dephosphorylated *β-catenin* is prevented and in presence of *Dvl* it translocates to the nucleus in Fig. 11*b*. The transition t10 shows the translocation of *β-catenin* to the nucleus by the high rate of *Dvl* as shown in Table 3.

The place *Axin* activates the places *GSK3* and *CK1* at t14 and t15 which in turn phosphorylates the *β-catenin* and results in *β-catenin* degradation (Figs. 14*a* and *b*) and hence causes the ventral fats. The places *GSK3* and *CK1* high transition rates at t16 in Table 4 inhibit place *Dvl* and proceeds the *β-catenin*

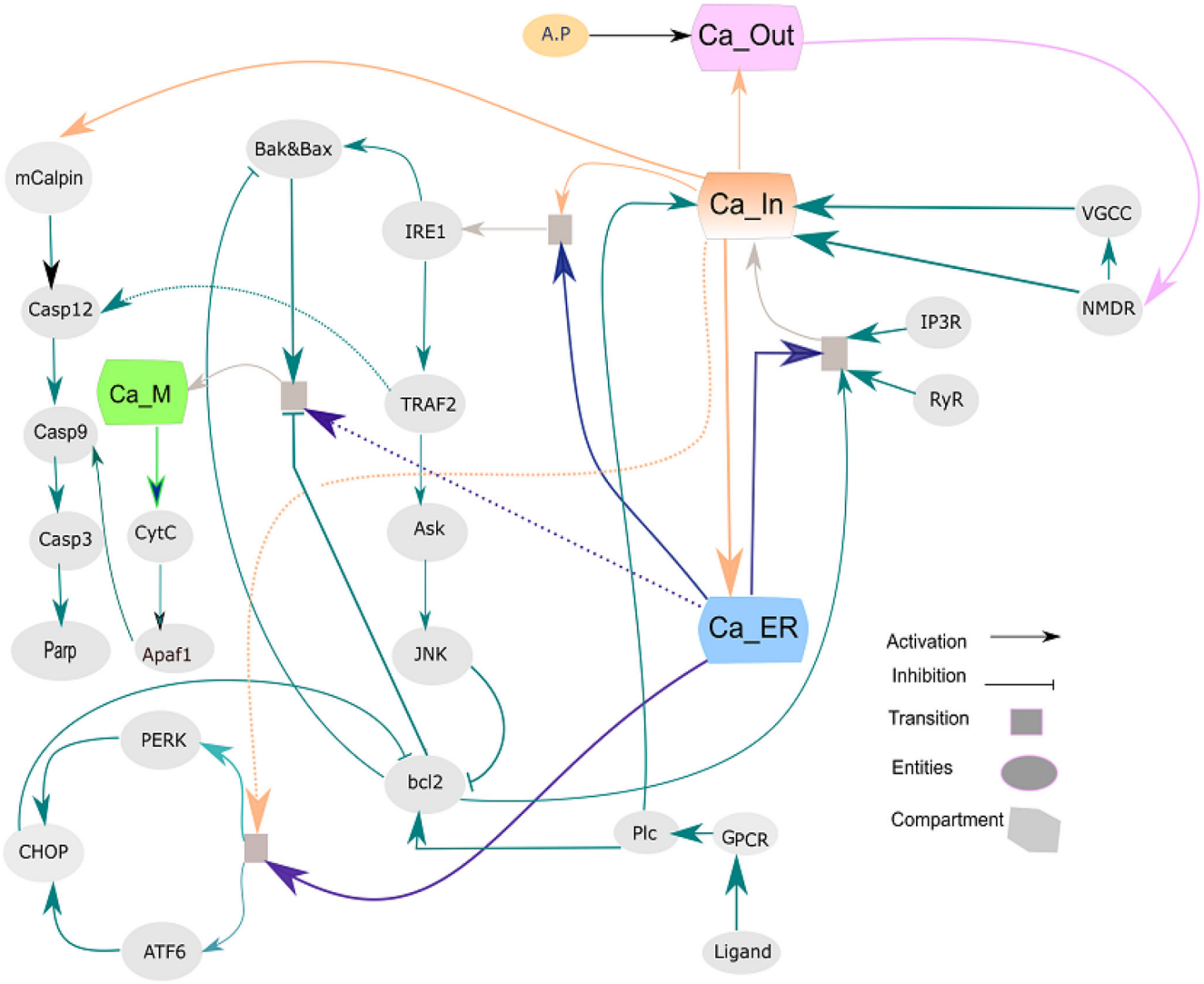


**Fig. 7** *Wnt*/$Ca^{2+}$ *signalling pathway shows calcium at different compartments as* $Ca^{2+}$ *in cytoplasm (Ca_in) presented by orange colour,* $Ca^{2+}$ *outside of cell (Ca_Out) by Violet colour,* $Ca^{2+}$ *in ER by Blue colour and* $Ca^{2+}$ *in mitochondria (Ca_M) by Green colour, respectively*

phosphorylation. Through t17, *axin* or *β-catenin* are not degraded in the presence of this *WLFA* complex. The *Tcf/lef* activates place *Axin* at transition t18.

The place *PP2A* inhibit *β-catenin* phosphorylation by suppression of place *GSK3* at transition t26 and place *PP1* dephosphorylates the *Axin* by suppression of *CK1* as presented in Figs. 15*a* and *b*. Furthermore, in the SPN model the place *APC* and *Axin* inhibit each other. The place *APC* inhibits the *PP2A* to regulate negatively the *β-catenin* degradation in Fig. 16*a*. The *Tcf/lef* activates place Axin at transition t18 which is presented in Fig. 16*b*. At t27 *CK1* is controlling *PP1* and *PP1* is recycled after it has degraded *CK1*. *Axin* is an inhibitor and *β-catenin* is degrading by *Axin* here inhibitor arc is not used to control both concentrations otherwise they will rise high. By t21, *PP2A* is activated in the absence of *APC*.

In Table 4 the high values of transitions show that these components recover the pathway from disease by decreasing values of inhibitors at low transition rates in the table.

The dephosphorylated *β-catenin* translocates to the nucleus and activates the place *Tcf/lef* which results in activation of *Wnt* responsive genes and suppresses the adipose tissues formation in cardiomyocytes. Hence activates the *Tcf/lef* and anti-apoptosis gene *Bcl2* by transition t25. Through t19 transition, the places *Axin* and *APC* activate each other. The transition t21 at a high rate as shown in Table 4 suppresses the *PP2A* place to promote *β-catenin* degradation. The t22 recycle to regulate the *PP2A*. When *β-catenin* is accumulated in the nucleus, the *Groucho* separates from *Tcf/lef* which results in activation of genes which positively regulates the *Wnt/β-catenin* signalling pathway through t10 and t23.

The *β-catenin* in absence of *Wnt* ligand make complex with *Axin, APC, GSK3* and *CK1* and phosphorylated by high transition rates of *GSK3* and *CK1* at transition t16, given in Table 4. *β-TrCP* causes the proteosomal degradation of *β-catenin* at transition t29. So the *Tcf/Groucho* represses *Wnt* target genes. The presence of *Wnt* disrupts *Axin* mediated degradation of *β-catenin* allowing the accumulation of *β-catenin* into the nucleus where it activates *Wnt* responsive genes through *Tcf/lef*. The *Nemo Like Kinase* inhibits the *Tcf/lef* at transition t24 to negatively regulates it.

*3.2.2 SPN models of* ***Wnt/***$Ca^{2+}$ *signalling:* The biological model of *Wnt*/$Ca^{2+}$ in Fig. 7 is converted into normal and pathological SPN model as presented in Figs. 9 and 10 respectively. The mass action rates of transitions of pathological SPN model (Table 5) are tuned according to the literature cited in Table 6. The SPN models in Figs. 9 and 10 show the $Ca^{2+}$ as *Ca_out (extracellular* $Ca^{2+}$*)*, *Ca_In (cytosolic_* $Ca^{2+}$*)*, *Ca_ER(*$Ca^{2+}$ *in ER store)* and *Ca_mito (*$Ca^{2+}$ *in mitochondria)*. The action potential makes the $Ca^{2+}$ enters to the cytoplasm by *VGCC* and *NMDR* channels, the *NCX* and *PMCA* show the efflux channels of $Ca^{2+}$. The $Ca^{2+}$ enters the cytoplasm which induces the release of $Ca^{2+}$ from ER and the depletion of $Ca^{2+}$ from ER cause the influx of $Ca^{2+}$ to ER [20].

The homeostatic SPN model is shown in Fig. 17*a* and the transitions rates in Table 6 shows that the extracellular $Ca^{2+}$ is more than the intracellular $Ca^{2+}$ but in the pathological model the

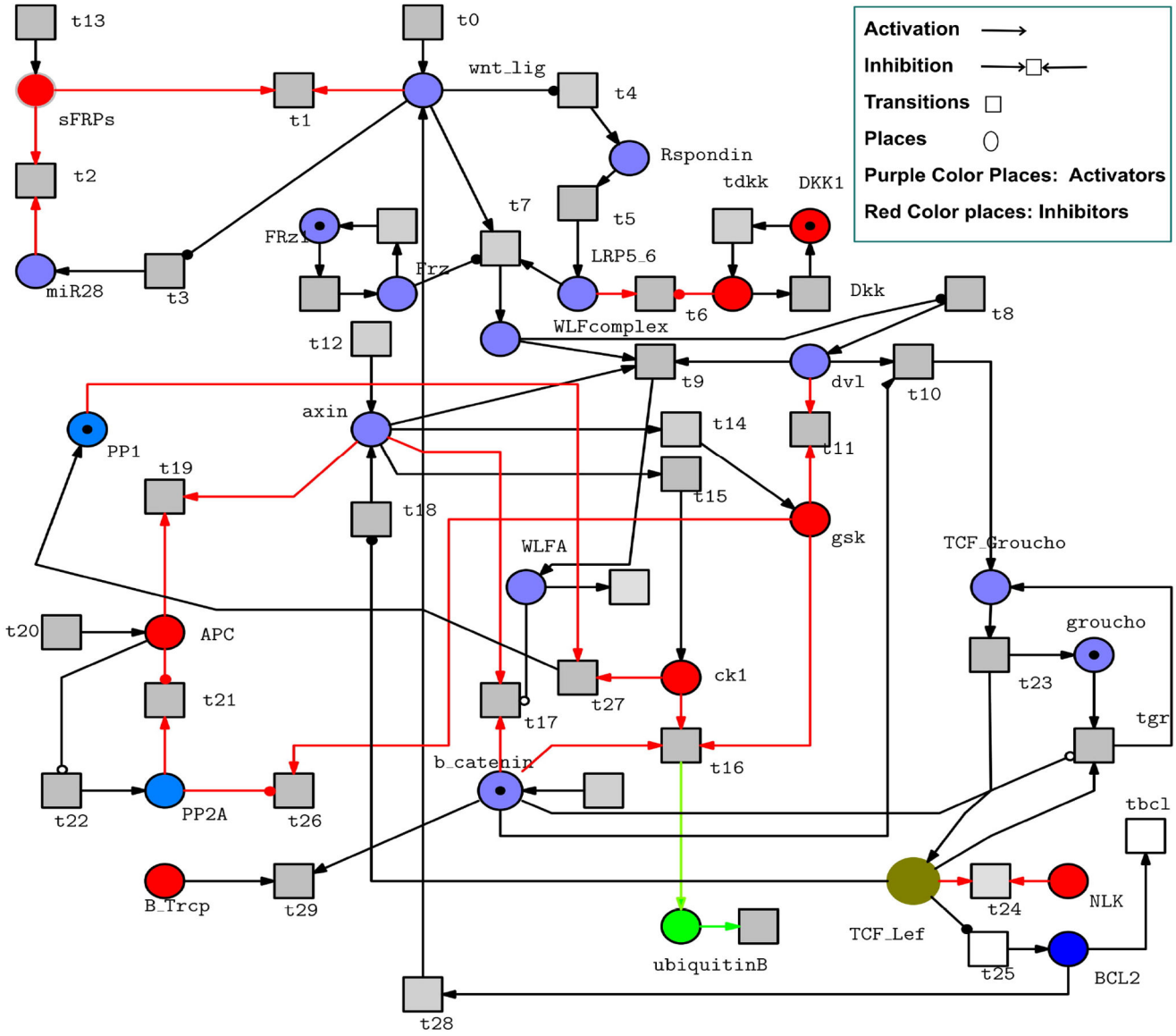


**Fig. 8** *Wnt/β-catenin SPN model shows that the Wnt signal keep GSK off and β-catenin translocate to nucleus to activate the Bcl2 gene by Tcf/lef. The PP1 and PP2A phosphatases in blue colour places are used as positive regulators to recover the pathway from disease state by inhibition of the GSK and Ck1 (its high transition rate leads the pathway to pathology)*

action potential increases the $Ca^{2+}$ influx to cytoplasm even more than extracellular $Ca^{2+}$ presented in Fig. 17*b*.

In SPN the ER stress is shown by places *IRE1*, *TRAF2*, *ASK* and *JNK*, and transitions (t40, t41, t42). The IRE1 activates *ASK*, *TRAF2* and *JNK,* respectively, where *JNK* inhibits the *Bcl2* at transition t43 by increasing the rate of transition to '1' shown in Table 5 which is pro-apoptotic component and presented in Fig. 18*a* [18]. The *bak&bax* is activated by *IRE1* at transition t44 which mediates mitochondrial apoptosis and *Bcl2* inhibits the *bak&bax* as shown in Fig. 18*b* [18].

The ER $Ca^{2+}$ overload also activates the *PERK* and *ATF* which further triggers the *CHOP* at transitions t45 and t46 having high rates of transitions in Table 5, which inhibit the *Bcl2* by t48 transition represented by Fig. 19*a*. The *Wnt* ligand activates the place *PLC* at t1 and *PLC* activate the place *Bcl2* at transition t37 which positively regulates the $Ca^{2+}$ homeostasis presented in Fig. 19*b*. So in the absence of *Wnt* ligand the $Ca^{2+}$ pathway will be dysregulated.

The increase of $Ca^{2+}$ in cytoplasm activates *mcalpain* at t59 high transition rate in Table 5 which mediates the apoptosis by activating *caspase12*, *caspase9*, *caspase3* and then *Parp* by (t60, t61 and t62, t63) finally cause apoptosis as shown in Fig. 20*a*. The $Ca^{2+}$ release from ER and moves into nearby mitochondria and the $Ca^{2+}$ elevation here rapture the mitochondrial membrane which releases the *cytochrome C* and $Ca^{2+}$ in the cytoplasm to mediates the apoptosis through *aPf1*, *caspse9*, *caspse3* to activate the pro-apoptotic component (*Parp*) by (t51, t52, t53, t54, t62 and t63) as presented in Fig. 20*b* [18].

The *Bcl2* inhibits the release of $Ca^{2+}$ from ER to Mitochondria and cytoplasm at transition t51 to decrease the $Ca^{2+}$ overload. Normally, the $Ca^{2+}$ moves out from mitochondria to ER at *NCLX* channel which is presented by transitions (t49 and t50) and its rates are shown in Table 5. The high level of $Ca^{2+}$ influx into cell deregulates the $Ca^{2+}$ homeostasis by creating stress as shown in Fig. 21.

The high level of extracellular $Ca^{2+}$ creates stress in cytoplasm through VGCC calcium channel shown in SPN model at transition t33 in Fig. 10. The cytoplasmic stress of $Ca^{2+}$ triggers the *RyRs* at ER where outflow of $Ca^{2+}$ occurs and $Ca^{2+}$ moves into cytoplasm as well as to mitochondria at t10 and t51, respectively. In both SPN models of *Wnt/β-catenin* and *Wnt*/$Ca^{2+}$ in Figs. 8 and 10, the *Wnt* ligand and *Bcl2* plays important role. The absence of *Wnt* ligand leads the pathway to disease state in both SPNs at transitions t1 in Figs. 8 and 10. The anti-apoptosis gene *Bcl2* in both SPNs used as therapeutic target. In *Wnt/β-catenin* as shown in Fig. 8, the *Bcl2* gene positively regulates the *Wnt* ligand in opposition of *sFRPs* inhibitor at transition t28. In Fig. 16 the SPN model of *Wnt*/$Ca^{2+}$, the *Bcl2* gene recover cell from the ER and mitochondrial $Ca^{2+}$

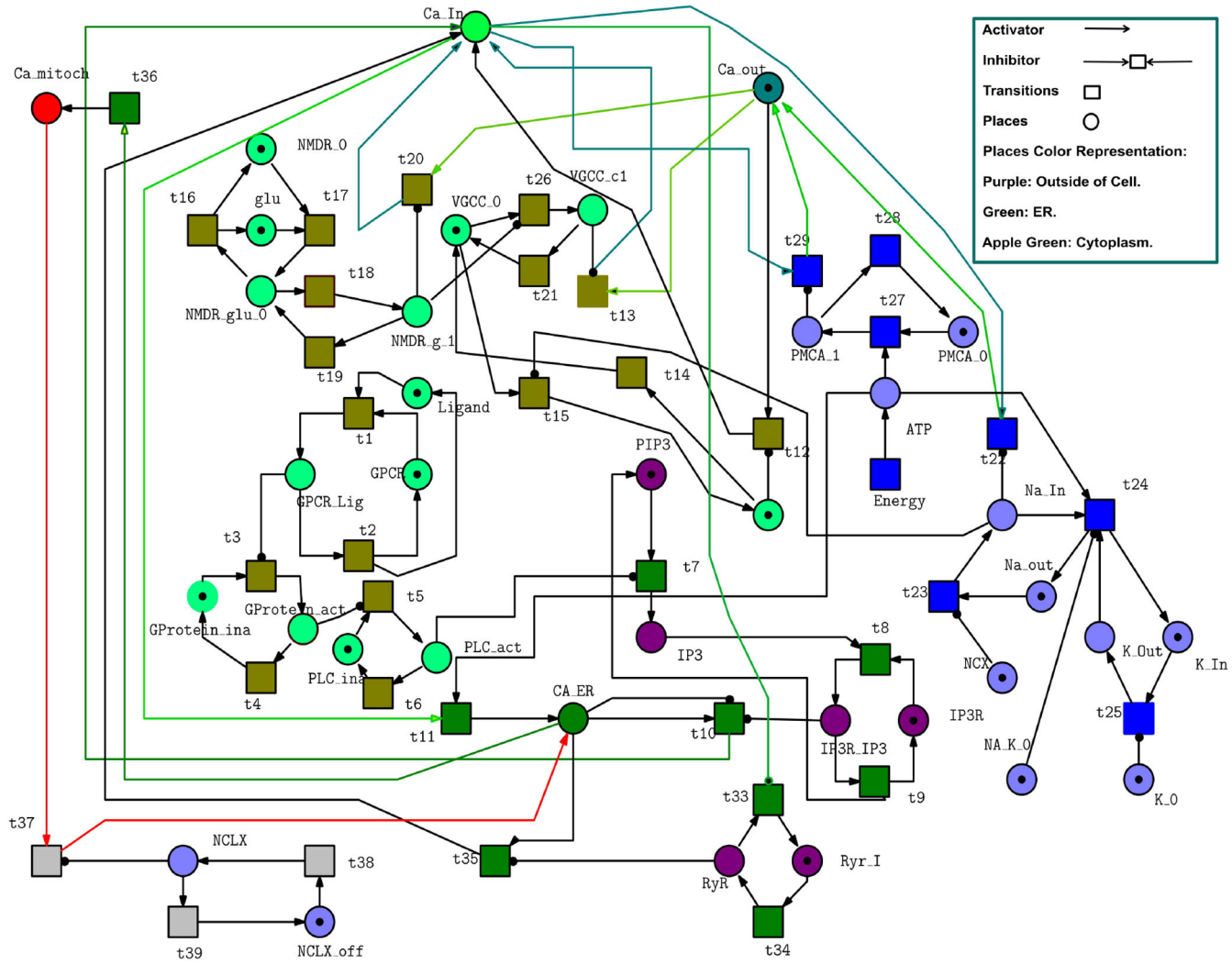


**Fig. 9** *SPN of Wnt/*$Ca^{2+}$ *homeostasis model, the red colour place in SPN shows the* $Ca^{2+}$ *in mitochondria. This model does not lead the signalling network towards the apoptotic pathway*

stress by inhibition of pro-apoptotic components *JNK* and *bak&bax*.

The *bak&bax* activates *mCalpain* in the cytoplasm at high transition rate in Table 5 having '1' value at t59 and regulates the pro-apoptotic component *mCalpain*, which is controlled by anti-apoptosis gene *Bcl2* as shown in Fig. 10. Moreover, the *TRAF2* also regulates the *Caspase12* at high transition rate of t58 in Table 5. Hence the *Bcl2* gene plays a vital role in *Wnt* signalling pathway for recovery from *ARVC* disease through prevention of adipose tissue formation in cardiomyocyte by positive feedback loops and inhibition of pro-apoptotic components.

## 4 Therapeutic intervention

The parameters in Table 3 illustrate the reaction rates where the tuning of the two important transitions, i.e. t12 and t13 show the degradation of *β-catenin* by entities *GSK3* and *CK1,* respectively. This tuning of parameters successfully allowed us to view how the progression of ARVC could be inhibited. In simulation graphs, it is observed that as the rate of transition t16 is decreased then the *β-catenin* level (shown in Fig. 13*b*) is increased in network and goes near the stability due to low activity of *GSK3*. Moreover, the rate of t13 (set to 0.01) increases the level of *β-catenin*. In Fig. 14*b*, both *GSK* and *CK1* level reduction results in increased *β-catenin* level which shows the dephosphorylation (De-pp) of *β-catenin* and its translocation to the nucleus as a result *Tcf/lef* is activated and prevents apoptosis. In Figs. 15(*a* and *b*, the phosphatases *PP2A* and *PP1* positively regulate the *Wnt* by inhibition of *GSK3* and *CK1* to prevent the *β-catenin* phosphorylation by them. The *PP1* and *PP2A* high transition rates such as 1 as shown in Table 3 make the reaction fast. The *Axin* and *APC* at transition at t19 regulate each other negatively which further suppress inhibition of *β-catenin* phosphorylation. Moreover, in the absence or decreased level of *Wnt* ligand the place *Rspondin* at transition t4 regulate the *Wnt* pathway as shown in Fig. 11*b*. *Tcf/lef* activate the *Bcl2* which is an anti-apoptosis gene and further in the ARVC pathway prevent adipose tissue formation in cardiomyocyte. The smaller level of Axin results in less amount of activation of *β-catenin* inhibitory components as *GSK* and *CK1,* which is maintained by *β-catenin* as shown in Fig. 13*b*.

The SPN model of *Wnt/*$Ca^{2+}$ in Fig. 10 shows that *JNK* inhibit anti apoptotic gene *Bcl2* at transition t43 by more cytoplasmic $Ca^{2+}$ because of action potential which causes ER stress as shown in Fig. 21 and mediate the mitochondrial apoptosis by transition t51 but the *PLC* at t37 which positively regulates *Bcl2* to suppress the activation of *JNK* and recover the $Ca^{2+}$ homeostasis to prevent ARVC. Overall these SPN models provide a good experimental platform to generate testable hypotheses and may aid in designing further experiments for therapeutic interventions. These models have also increased our comprehension towards understanding the underlying mutual dynamics of the two important signalling pathways in pathophysiology of ARVC.

## 5 Conclusion

In ARVC, *β-catenin* has a central role as it degrades and creates adipose tissues in cardiomyocyte. The fatty tissues formed from ubiquitination of degraded *β-catenin* by bTrcp in *Wnt* signalling pathway. The development of a given pathological pathway increases due to activation of *GSK3* and *CK1*. These inhibitors

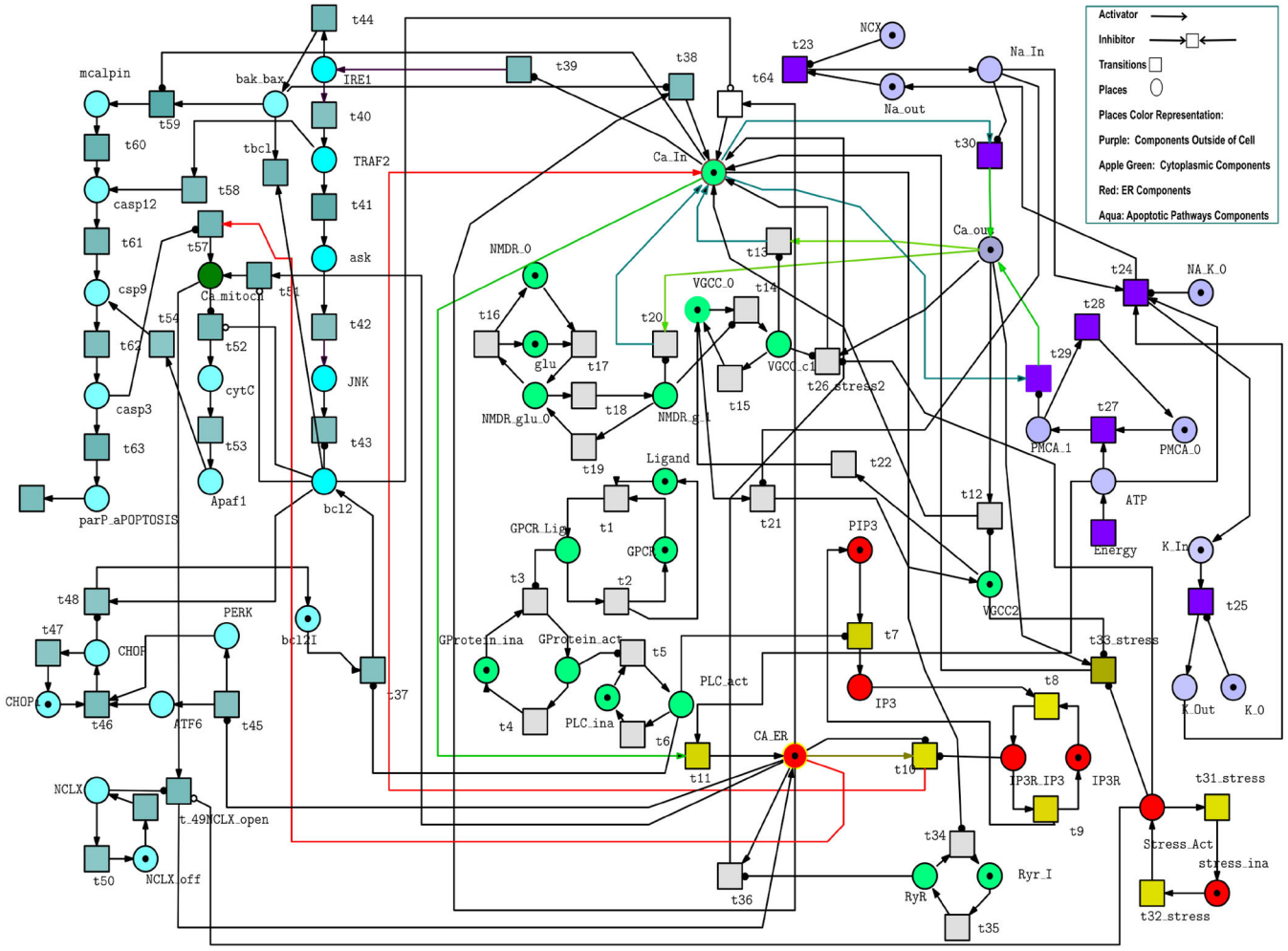


**Fig. 10** *SPN model of Wnt/*$Ca^{2+}$ *for ARVC, this SPN shows the* $Ca^{2+}$ *overload in cytoplasm and ER stress activates the apoptotic pathway by (IRE1, ASK, TRAF2, JNK to inhibit the Bcl2) which further leads to mitochondrial apoptosis through activation of caspases and mCalpain*

**Table 1** Summary of comparison between reported experimental observations and simulation results for Wnt/*β*-catenin Signalling

| S.No | Observations | Experimental findings | Model simulation | Citations |
|---|---|---|---|---|
| 01 | effect of Dikk0pf binding with LRP5/6 on Wnt signalling | — | — | [38] |
| 02 | *Wnt signalling effects GSK3 via Dvl* | — | — | [39, 40] |
| 03 | *Gkk3 and Ck1 effects b-catenin translocation to nucleus causes ARVC* | — | — | [41] |
| 04 | *Axin effects**** β-catenin degradation* | + | + | [42, 43] |
| 05 | effect of Bcl2 gene on Wnt signalling | + | + | [44] |

**Table 2** Summary of comparison between reported experimental observations and simulation results for $Wnt/Ca^{2+}$ Signalling

| S.no | Observations | Experimental finding | Model simulations | Citations |
|---|---|---|---|---|
| 01 | effect of JNK on Bcl2 causes ARVC | — | — | [45–47] |
| 02 | *Bcl2* gene effect on mitochondrial $Ca^{2+}$ overload | — | — | [47, 48] |
| 03 | *Bcl2* effect on bak&bax in down regulation of apoptosis | + | + | [47] |
| 04 | *CHOP* down regulates *Bcl2* causes *ARVC* | — | — | [47, 49] |
| 05 | ER stress promotes the $Ca^{2+}$ overload in cytosol which causes apoptosis | + | + | [50] |
| 06 | effect of $Ca^{2+}$ signalling on apoptosis (ARVC) | + | + | [8, 51] |
| 07 | $Ca^{2+}$ influx upregulate calpain and induce apoptosis | + | + | [51, 52] |

trigger the suppression of *β-catenin* De-pp. In SPN model all these observations were implanted and analysed. The ARVC mechanism is explained and we were able to derive some meaningful observations. The first important observation is the low level of *Dvl* in the absence of Wnt ligand dysregulates the *Wnt* pathway and *β-catenin* starts to degrade gradually. The high rate of inhibitor *DKK* also suppresses the *LRP5/6* receptor to stop composition of *Wnt/Frizz* complex that further activates the pathway. The regulator *Rspondin* of *Wnt/β-catenin* pathway, which regulates the pathway in the absence or low rate of *Wnt* ligand. Except that the *PP1* and *PP2A* phosphatases also regulate the *β-catenin* De-pp in a positive feedback loop. The second important observation is when *β-catenin* accumulates in the nucleus and associate with *Tcf/lef* to activate anti-apoptosis genes and *Wnt* responsive genes to positively regulate the *Wnt* signalling pathway and also interlinked pathways to reduce the progression of ARVC.

**Table 3** Transition rates of SPN model of Wnt/$\beta$-catenin regulatory system during homeostasis

| Transitions | Rate, $\mu$ | Transitions | Rate, $\mu$ |
|---|---|---|---|
| t1 | 0.1 | t15 | 0.5 |
| t2 | 1 | t16 | 0.01 |
| t3 | 1 | t17 | 1 |
| t4 | 1 | t18 | 1 |
| t5 | 1 | t19 | 0.5 |
| t6 | 0.01 | t20 | 1 |
| t7 | 1 | t21 | 0.5 |
| t8 | 1 | t22 | 0.1 |
| t9 | 1 | t23 | 1 |
| t10 | 10 | t24 | 0.5 |
| t11 | 1 | t25 | 1 |
| t12 | 1 | t26 | 0.1 |
| t13 | 0.01 | t27 | 0.1 |
| t14 | 0.5 | t28 | 1 |

**Table 4** Transition rates of SPN model of Wnt/$\beta$-catenin during ARVC

| Transitions | Rate, $\mu$ | Transitions | Rate, $\mu$ |
|---|---|---|---|
| t1 | 1 | t15 | 1 |
| t2 | 0.5 | t16 | 1 |
| t3 | 0.5 | t17 | 0.1 |
| t4 | 1 | t18 | 0.1 |
| t5 | 0.1 | t19 | 1 |
| t6 | 1 | t20 | 1 |
| t7 | 0.1 | t21 | 1 |
| t8 | 0.1 | t22 | 1 |
| t9 | 0.1 | t23 | 0.1 |
| t10 | 0.1 | t24 | 1 |
| t11 | 0.01 | t25 | 1 |
| t12 | 1 | t26 | 1 |
| t13 | 1 | t27 | 1 |
| t14 | 1 | t28 | 0.1 |

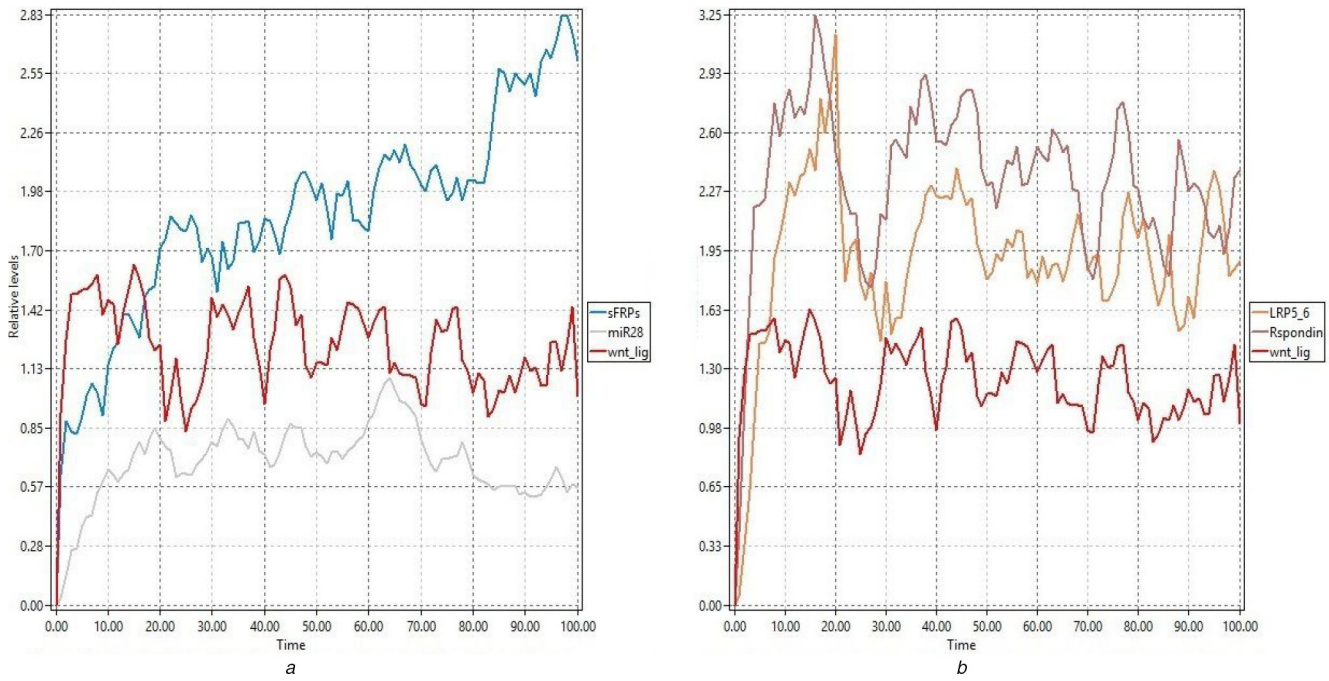


**Fig. 11** *Up regulation and down regulation of Wnt ligand*

***(a)*** In the presence of sFRPs inhibitor, the Wnt ligand and the miR28 (which positively regulate the ligand) both are suppressed, ***(b)*** Wnt ligand is regulated positively by activators LRP 5/6 and Rspondin

The interlinked pathway of *Wnt/β-catenin* is $Ca^{2+}$ signalling pathway where the action potential influx more $Ca^{2+}$ into cytosol and initiate the ER stress which further mediate the mitochondrial apoptosis. The ER stress activates *IRE1, TRAF2, ASK* and *JNK*

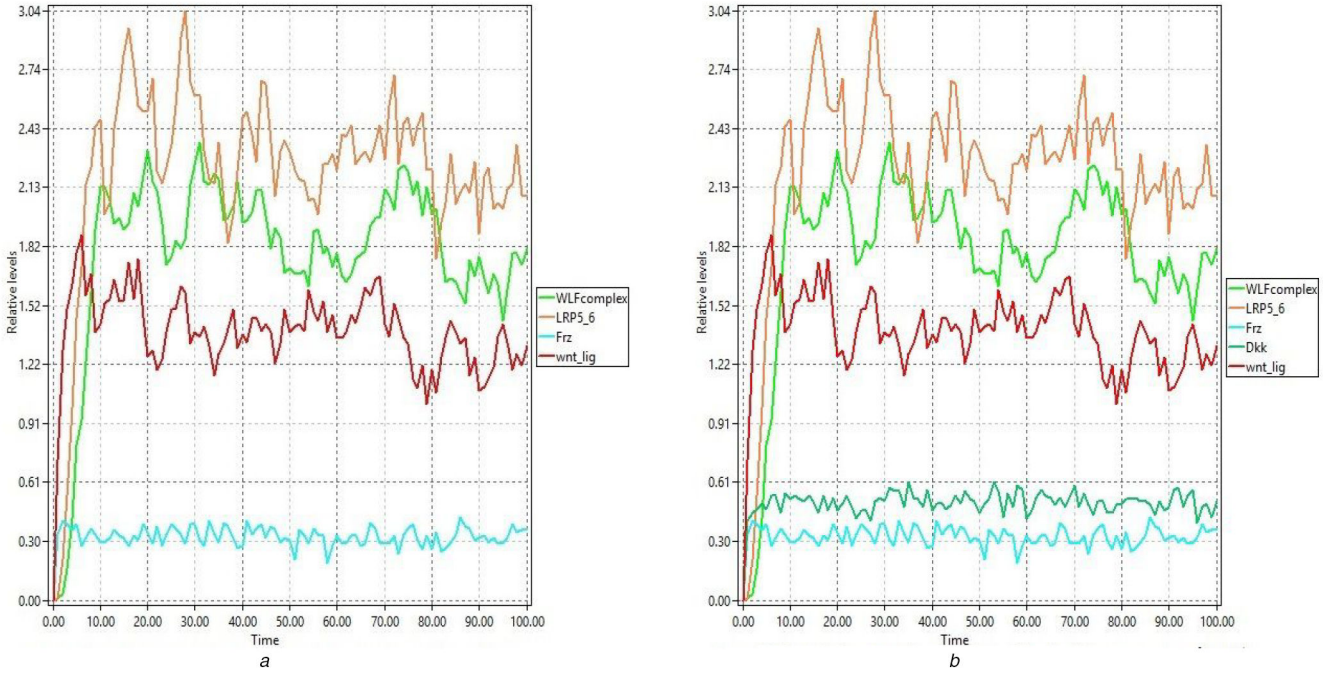


**Fig. 12** *The Wnt/Frizz inhibition and activation*

***(a)*** In the presence of Wnt and LRP5/6 the complex Wnt/frizz value is increased, ***(b)*** Inhibitor DKK lowered the Wnt/frizz level by supression of LRP5/6 activator

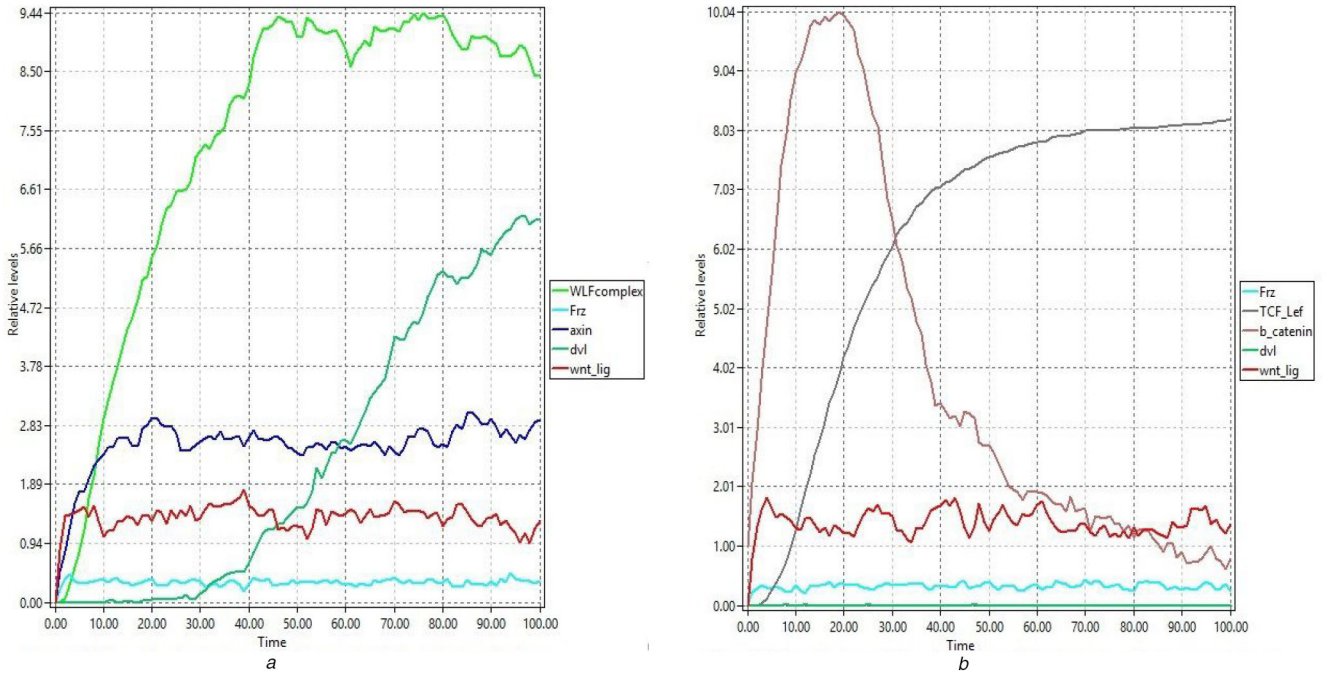


**Fig. 13** *Inhibition of β-catenin degradation*

***(a)*** Wnt/frizz complex activates Dvl and dephosphorylates *β*-catenin, ***(b)*** Activation of Dvl and inhibition of *β*-catenin degradation shows its binding with Tcf/lef

which inhibit the *Bcl2*. In result more $Ca^{2+}$ from ER and cytosol moves into Mitochondria to cause apoptosis and also the increase of intracellular $Ca^{2+}$ activates the mcalpain which activates caspase, cascade to cause ARVC pathology. Here in $Ca^{2+}$ signalling pathway the *Bcl2* which maintain the $Ca^{2+}$ regulation system by suppressing *JNK* and *PLC* is the main positive regulator of *Bcl2*. By considering these observations, better therapeutic interventions are warranted upon further pursual in wet lab experiments. We also aim to extend this work by constructing automata network models of the *Wnt/β-catenin* and *Wnt*/$Ca^{2+}$ for the identification of stable states and biomarkers.

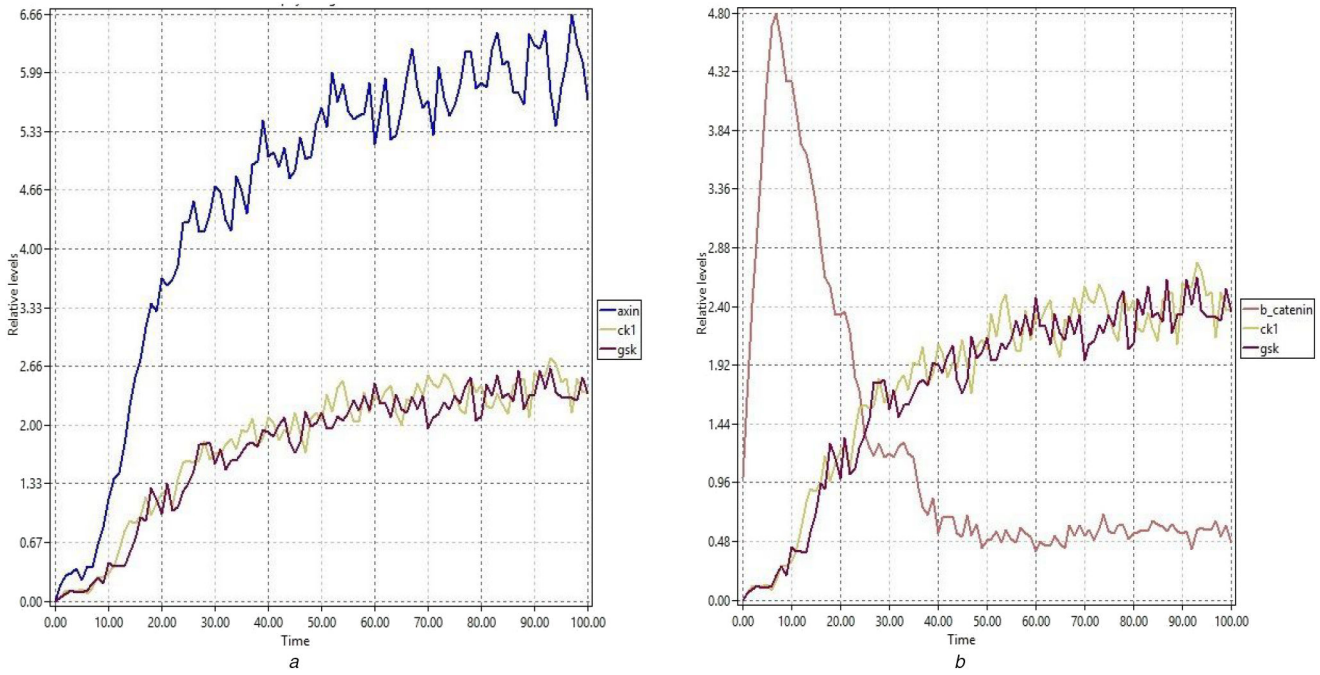


**Fig. 14** *Degradation of β-catenin*
***(a)*** Ck1 and GSK3 are activated by axin, ***(b)*** Ck1 and GSK3 degraded the *β*-catenin

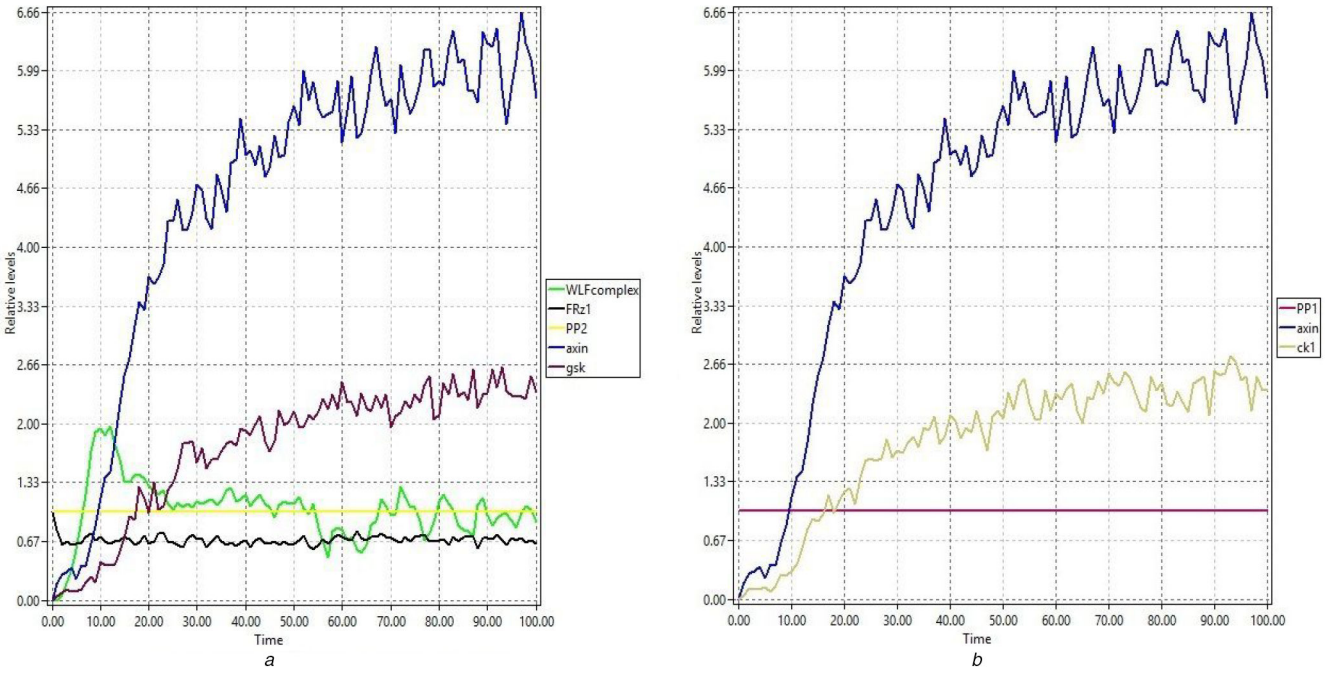


**Fig. 15** *Down regulation of β-catenin phosphorylation*
***(a), (b)*** PP2A inhibits the GSK3 and PP1 inhibits CK1 to reverse the *β*-catenin phosporylation

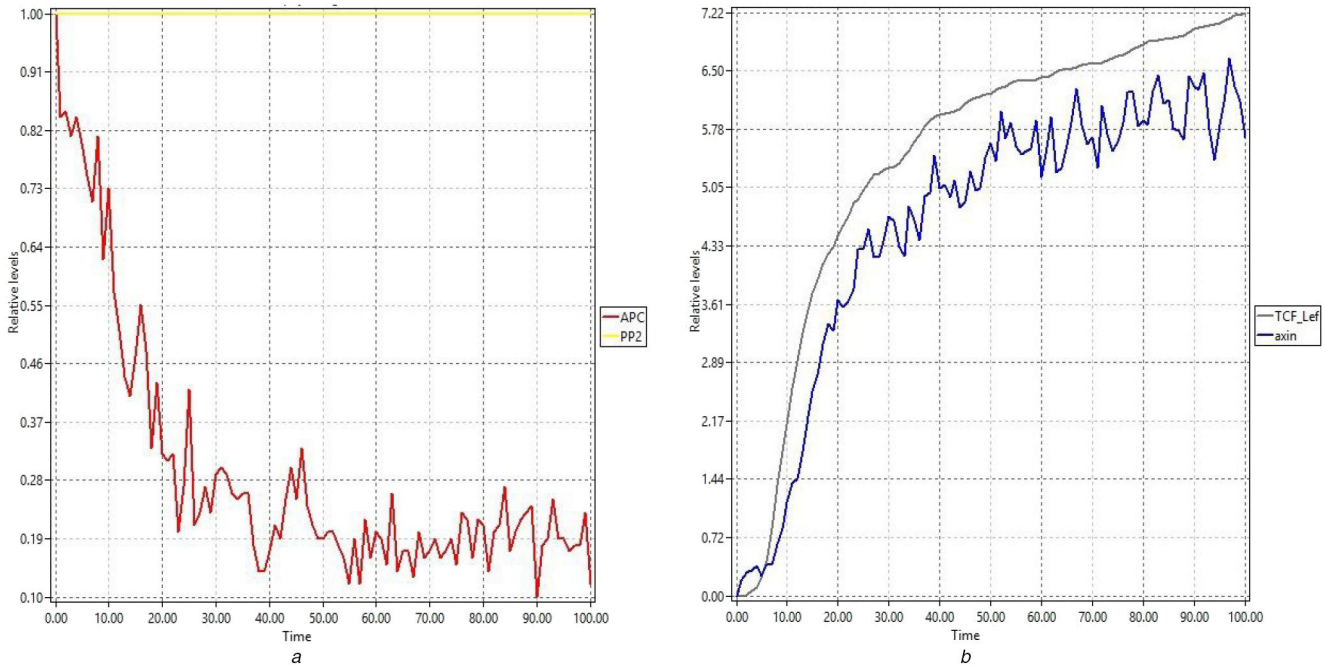


**Fig. 16** *Up and down regulation of Axin*
***(a)*** PP2A and APC negatively regulate each other, ***(b)*** Tcf/lef regulates positively the Axin

**Table 5** Transition rates of *Wnt*/$Ca^{2+}$ pathological model

| Transitions | Rate, $\mu$ | Transitions | Rate, $\mu$ |
|---|---|---|---|
| t38 | 0.1 | t51 | 1 |
| t39 | 0.01 | t52 | 1 |
| t40 | 0.1 | t53 | 1 |
| t41 | 0.1 | t54 | 1 |
| t42 | 0.01 | t55 | 1 |
| t43 | 0.1 | t56 | 1 |
| t44 | 0.1 | t57 | 1 |
| t45 | 1 | t58 | 1 |
| t46 | 0.01 | t59 | 1 |
| t47 | 1 | t60 | 1 |
| t48 | 1 | t61 | 1 |
| t49 | 1 | t62 | 1 |
| t50 | 1 | t63 | 1 |

**Table 6** Transition rates of Wnt/$Ca^{2+}$ homeostatic model

| Transitions | Rate, $\mu$ | Transitions | Rate, $\mu$ |
|---|---|---|---|
| t1 | 1 | t20 | 1 |
| t2 | 1 | t21 | 1 |
| t3 | 1 | t22 | 1 |
| t4 | 1 | t23 | 1 |
| t5 | 1 | t24 | 0.1 |
| t6 | 1 | t25 | 1 |
| t7 | 1 | t26 | 1 |
| t8 | 1 | t27 | 1 |
| t9 | 1 | t28 | 1 |
| t10 | 1 | t29 | 1 |
| t11 | 1 | t30 | 1 |
| t12 | 1 | t31 | 1 |
| t13 | 1 | t32 | 0.1 |
| t14 | 1 | t33 | 1 |
| t15 | 0.1 | t34 | 1 |
| t16 | 1 | t35 | 1 |
| t17 | 1 | t36 | 1 |
| t18 | 1 | t37 | 1 |
| t19 | 1 | t38 | 1 |

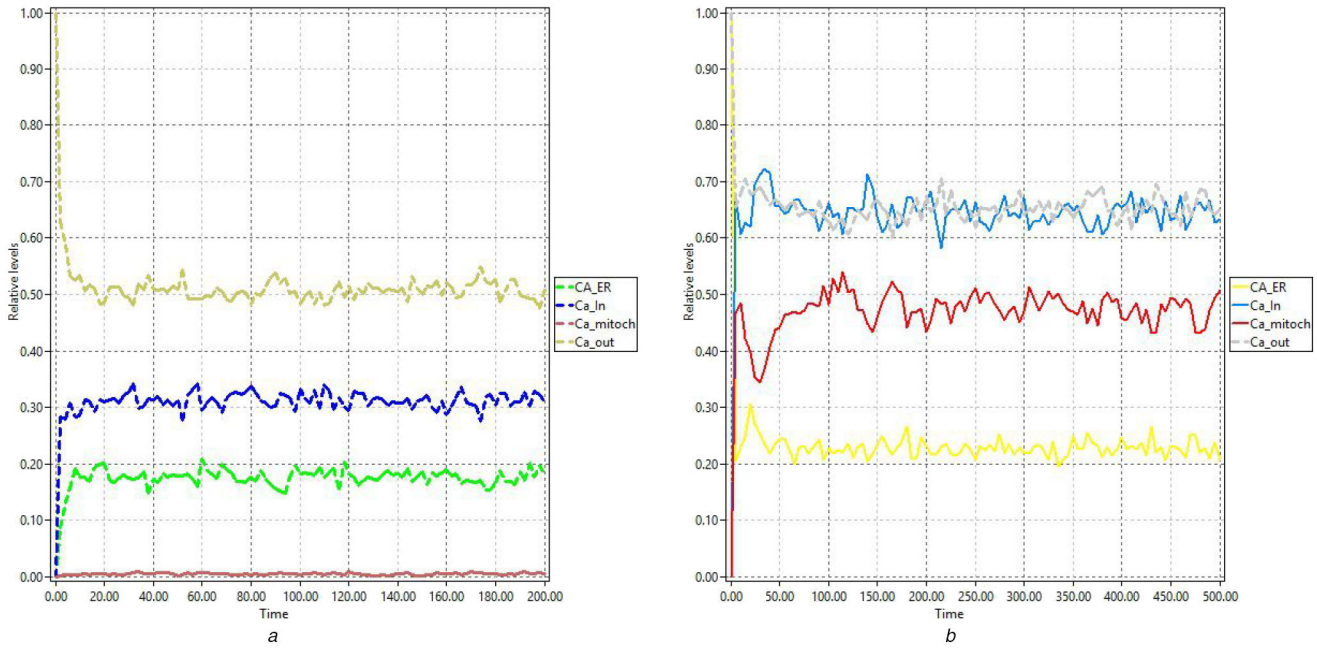


**Fig. 17** *The $Ca^{2+}$ homeostasis and dysregulation of homeostasis in many compartments of cardiomyocyte*
***(a)*** Shows the normal Ca_in and Ca out, Ca_ER and Ca_mitochondria, ***(b)*** Shows the action potential increased the Ca_in so much even more than Ca_out

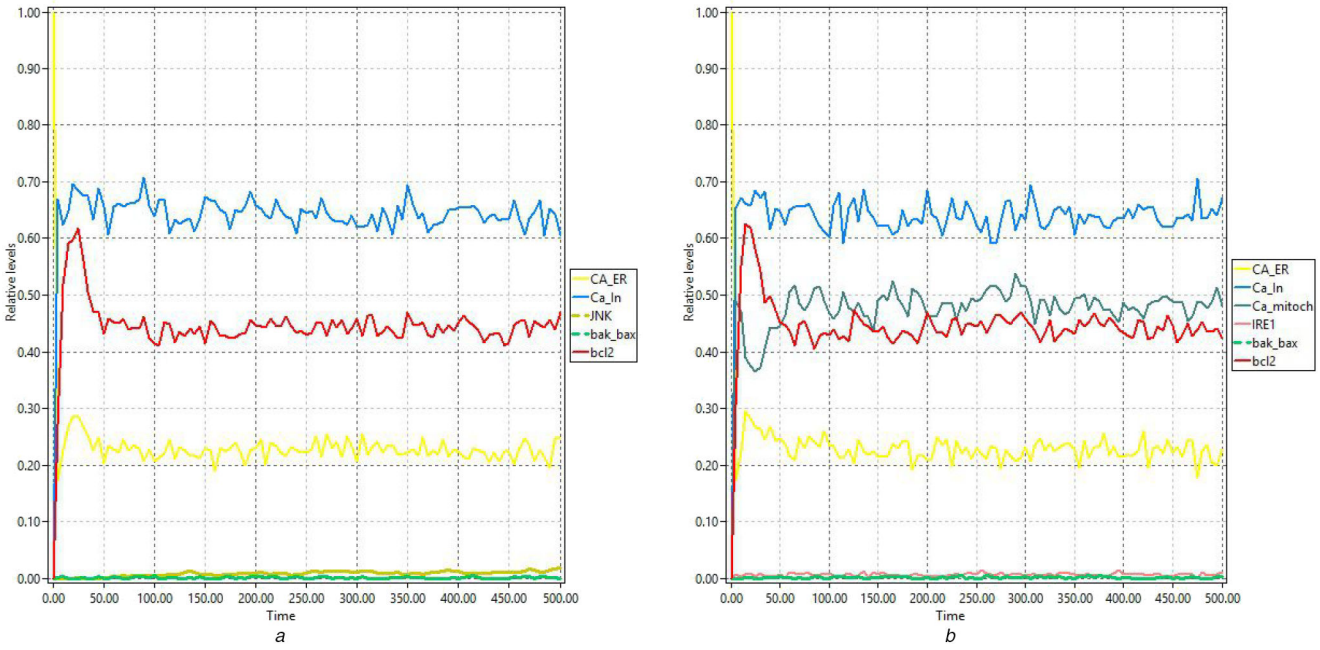


**Fig. 18** *The activation of Apoptotic pathways and its inhibition by Bcl2*
***(a)*** Increase of Ca-ER, C-In activates the IRE1 which activates ASK, TRAF, JNK and JNK inhibit the Bcl2 and vice versa, ***(b)*** Decrease of Ca_ER and Ca_In activates the Bcl2 and Bcl2, inhibits the bak&bax and lowers the level of $Ca^{2+}$ in mitochondria

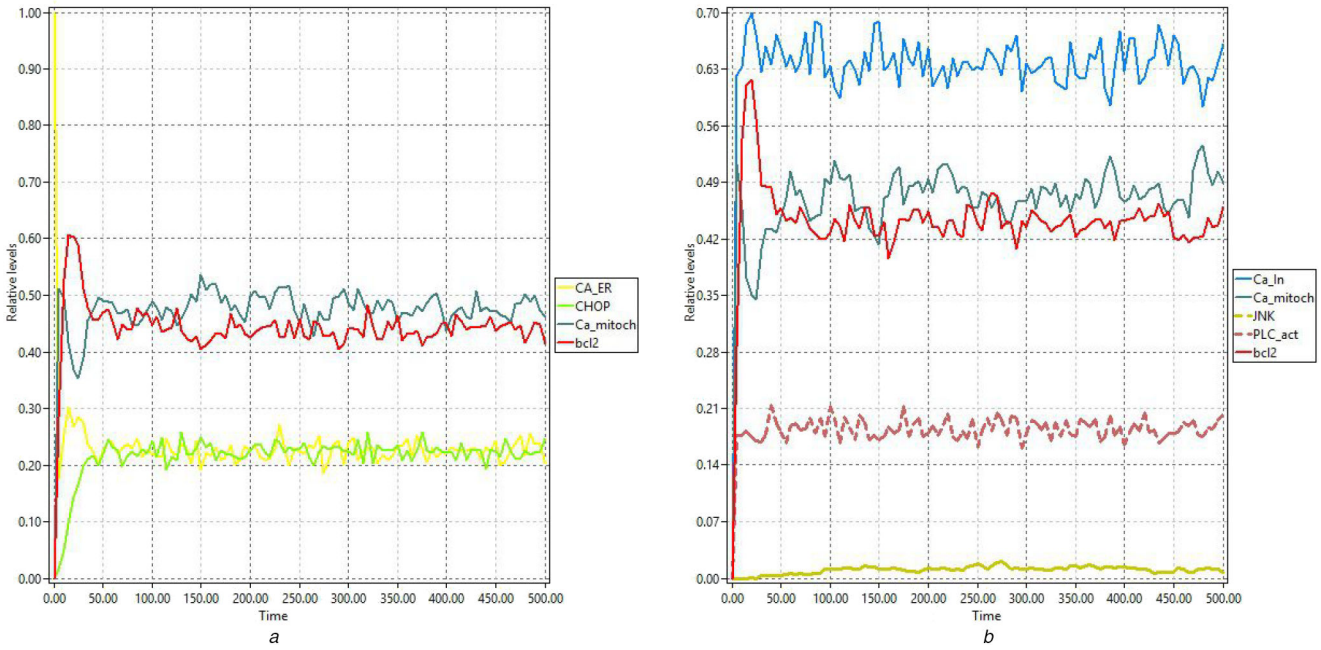


**Fig. 19** *The effect of Bcl2 on Mitochondrial and ER $Ca^{2+}$ regulation*

***(a)*** Increase of CHOP decreases Bcl2 level increases the $Ca^{2+}$ in mitochondria, ***(b)*** In the presence of PLC the Bcl2 increases which inhibits the JNK and vice versa

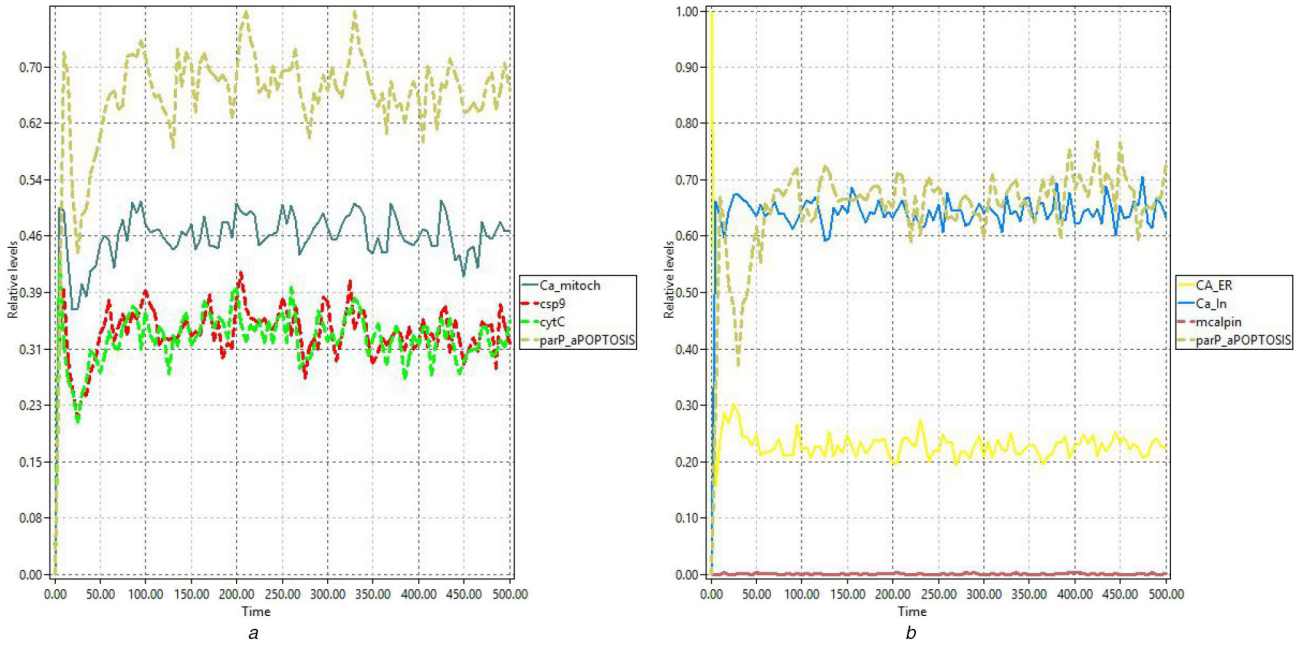


**Fig. 20** *Mitochondrial Apoptosis*

***(a)*** Ca_ER and bak&bax release calcium into mitochondria (Ca mito) which release the cytc into the cytoplasm and activates the Casp9, Casp3 and then Parp (pro-apoptosis), the NCLX move calcium out of mitochondria into ER in the normal way (not in pathology), ***(b)*** Increase of $Ca^{2+}$ in ER and cytoplasm activates the mCalpain, which activates the caspase cascade and rises the level of parP_aPOPTOSIS

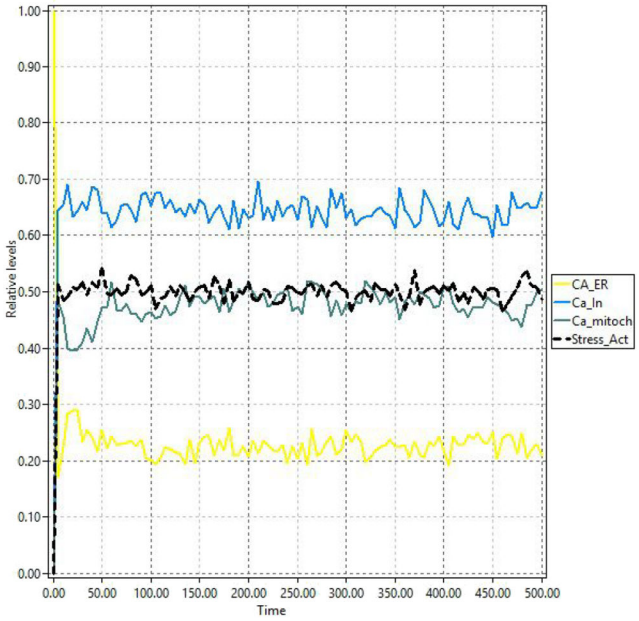


**Fig. 21** *Stress created by* $Ca^{2+}$ *high-level outside increases the Ca_in, Ca_ER and Ca_mitochondria*

## 6 References


[1] van Tintelen, J.P., Hofstra, R.M., Wiesfeld, A.C., *et al.*: 'Molecular genetics of arrhythmogenic right ventricular cardiomyopathy: emerging horizon?', *Curr. Opin. Cardiol.*, 2007, **22**, (3), pp. 185–192

[2] Basso, C., Corrado, D., Bauce, B., *et al.*: 'Arrhythmogenic right ventricular cardiomyopathy', *Circul.: Arrhythmia Electrophysiol.*, 2012, **5**, (6), pp. 1233–1246

[3] Lluri, G., Deb, A.: 'Wnt signaling and cardiac fibrosis', in Willis, M., Yates, C.C., Schisler, J.C. (Eds.): '*Fibrosis in disease*' (Springer, Heidelberg, Germany, 2019), pp. 319–334

[4] Austin, K.M., Trembley, M.A., Chandler, S.F., *et al.*: 'Molecular mechanisms of arrhythmogenic cardiomyopathy', *Nat. Rev. Cardiol.*, 2019, **16**, (9), pp. 519–537

[5] Ravi, S., Willis, M.S., Schisler, J.C.: 'Fibrotic signaling in cardiomyopathies', in Willis, M., Yates, C.C., Schisler, J.C. (Eds.): '*Fibrosis in disease*' (Springer, Heidelberg, Germany, 2019), pp. 273–317

[6] AlTurki, A., Alotaibi, B., Joza, J., *et al.*: 'Arrhythmogenic right ventricular cardiomyopathy/dysplasia: mechanisms and management', *Res. Reports Clin. Cardiology*, 2020, **11**, p. 19

[7] Stevens, T.L., Wallace, M.J., Refaey, M.E., *et al.*: 'Arrhythmogenic cardiomyopathy: molecular insights for improved therapeutic design', *J. Cardiovasc. Dev. Dis.*, 2020, **7**, (2), p. 21

[8] Moccia, F., Lodola, F., Stadiotti, I., *et al.*: 'Calcium as a key player in arrhythmogenic cardiomyopathy: adhesion disorder or intracellular alteration?', *Int. J. Mol. Sci.*, 2019, **20**, (16), p. 3986

[9] Tareen, S.H.K., Ahmad, J.: 'Modelling and analysis of the feeding regimen induced entrainment of hepatocyte circadian oscillators using Petri nets', *PloS One*, 2015, **10**, (3), p. e0117519

[10] Bibi, Z., Ahmad, J., Paracha, R.Z., *et al.*: 'Modeling and analysis of the signaling crosstalk of pi3k, ampk and MAPK with timed hybrid Petri nets approach'. 2017 17th Int. Conf. on Computational Science and Its Applications (ICCSA), Trieste, Italy, 2017, pp. 1–7

[11] Sheikh, I. A., Ahmad, J., Saeed, M. T.: 'Modelling and simulation of biological regulatory networks by stochastic Petri nets'. Proc. of the World Congress on Engineering and Computer Science, San Francisco, USA, 2016, vol. 2

[12] Siddiqa, A., Ahmad, J., Ali, A., *et al.*: 'Deciphering the expression dynamics of angptl8 associated regulatory network in insulin resistance using formal modelling approaches', *IET Syst. Biol.*, 2020, **14**, (2), pp. 47–58

[13] Huelsken, J., Behrens, J.: 'The wnt signalling pathway', *J. Cell Sci.*, 2002, **115**, (21), pp. 3977–3978

[14] Harvey, P., Leinwand, L.: 'The cell biology of disease: cellular mechanisms of cardiomyopathy', *J. Cell Biol.*, 2011, **194**, pp. 355–365

[15] Lorenzon, A., Calore, M., Poloni, G., *et al.*: 'Wnt/$\beta$-catenin pathway in arrhythmogenic cardiomyopathy', *Oncotarget*, 2017, **8**, (36), p. 60640

[16] MacDonald, B.T., Tamai, K., He, X.: 'Wnt/$\beta$-catenin signaling: components, mechanisms, and diseases', *Dev. Cell*, 2009, **17**, (1), pp. 9–26

[17] Kühl, M., Sheldahl, L.C., Malbon, C.C., *et al.*: '$Ca^{2+}$/calmodulin-dependent protein kinase ii is stimulated by wnt and frizzled homologs and promotes ventral cell fates in xenopus', *J. Biol. Chem.*, 2000, **275**, (17), pp. 12701–12711

[18] Bahar, E., Kim, H., Yoon, H.: 'Er stress-mediated signaling: action potential and $Ca^{2+}$ as key players', *Int. J. Mol. Sci.*, 2016, **17**, (9), p. 1558

[19] Chung, W.Y., Jha, A., Ahuja, M., *et al.*: '$Ca^{2+}$ influx at the er/pm junctions', *Cell Calcium*, 2017, **63**, pp. 29–32

[20] Ashraf, J., Ahmad, J., Ali, A., *et al.*: 'Analyzing the behavior of neuronal pathways in alzheimer's disease using Petri net modeling approach', *Front. Neuroinform.*, 2018, **12**, p. 26

[21] Brauer, W., Reisig, W.: 'Carl adam Petri and Petri nets', *Fundam. Concepts Comput. Sci.*, 2009, **3**, (5), pp. 129–139

[22] Polak, M. E., Ung, C. Y., Masapust, J., *et al.*: 'Petri net computational modelling of langerhans cell interferon regulatory factor network predicts their role in t cell activation', *Sci. Rep.*, 2017, **7**, (1), p. 668

[23] Napione, L., Manini, D., Cordero, F., *et al.*: 'On the use of stochastic Petri nets in the analysis of signal transduction pathways for angiogenesis process'. Int. Conf. on Computational Methods in Systems Biology, Bologna, Italy, 2009, pp. 281–295

[24] Mehraei, M., Sadr, H.: 'Identifying potential gene therapy to treat glioblastoma through inhibition of the pi3k/akt/mtor signaling pathway using fuzzy stochastic hybrid functional Petri nets', *J. Modern Technol. Eng.*, 2020, **5**, (1), pp. 18–24

[25] Ahmadian, M., Tyson, J.J., Peccoud, J., *et al.*: 'A hybrid stochastic model of the budding yeast cell cycle', *NPJ Syst. Biol. Appl.*, 2020, **6**, (1), pp. 1–10

[26] Valk, R.: 'On the two worlds of carl adam petris nets', in Reisig, W., Rozenberg, G. (Eds.): '*Carl adam Petri: ideas, personality, impact*' (Springer, Heidelberg, Germany, 2019), pp. 37–44

[27] Reisig, W., Rozenberg, G.: '*Lectures on Petri nets i: basic models: advances in Petri nets*' (Springer Science & Business Media, Heidelberg, Germany, 1998)

[28] Blätke, M. A., Heiner, M., Marwan, W.: 'Petri nets in systems biology', Technical Report, Otto-von-Guericke University Magdeburg, Tech. Rep., 2011

[29] Heiner, M., Gilbert, D., Donaldson, R.: 'Petri nets for systems and synthetic biology', in Bernardo, M., Degano, P., Zavattaro, G. (Eds.): '*International school on formal methods for the design of computer, communication and software systems*' (Springer, Heidelberg, Germany, 2008), pp. 215–264

[30] Niarakis, A., Thieffry, D.: 'Logical modelling of cellular networks', 2018

[31] Livigni, A., O'Hara, L., Polak, M.E., *et al.*: 'A graphical and computational modeling platform for biological pathways', *Nat. Protoc.*, 2018, **13**, (4), pp. 705–722

[32] Balazki, P., Lindauer, K., Einloft, J., *et al.*: 'Monalisa for stochastic simulations of Petri net models of biochemical systems', *BMC Bioinformatics*, 2015, **16**, (1), p. 215

[33] Heiner, M., Richter, R., Schwarick, M., *et al.*: 'Snoopy-a tool to design and execute graph-based formalisms', *Petri Net Newsletter*, 2008, **74**, pp. 8–22

[34] David, R., Alla, H.: '*Discrete, continuous, and hybrid Petri nets*' (Springer, Heidelberg, Germany, 2005), vol. **1**

[35] Heiner, M., Herajy, M., Liu, F., *et al.*: 'Snoopy–a unifying Petri net tool'. Int. Conf. on Application and Theory of Petri Nets and Concurrency, Hamburg, Germany, 2012, pp. 398–407

[36] Meng, T. C., Somani, S., Dhar, P.: 'Modeling and simulation of biological systems with stochasticity', *Silico Biol.*, 2004, **4**, (3), pp. 293–309

[37] Rohr, C., Marwan, W., Heiner, M.: 'Snoopy, a unifying Petri net framework to investigate biomolecular networks', *Bioinformatics*, 2010, **26**, (7), pp. 974–975

[38] Ahn, V.E., Chu, M.L.-H., Choi, H.-J., *et al.*: 'Structural basis of wnt signaling inhibition by dickkopf binding to lrp5/6', *Dev. Cell*, 2011, **21**, (5), pp. 862–873

[39] Metcalfe, C., Bienz, M.: 'Inhibition of GSK3 by wnt signalling–two contrasting models', *J. Cell Sci.*, 2011, **124**, (21), pp. 3537–3544

[40] Wu, D., Pan, W.: 'Gsk3: a multifaceted kinase in wnt signaling', *Trends Biochem. Sci.*, 2010, **35**, (3), pp. 161–168

[41] Stamos, J.L., Weis, W.I.: 'The $\beta$-catenin destruction complex', *Cold Spring Harbor Perspect. Biol.*, 2013, **5**, (1), p. a007898

[42] Song, X., Wang, S., Li, L.: 'New insights into the regulation of axin function in canonical wnt signaling pathway', *Protein Cell.*, 2014, **5**, (3), pp. 186–193
[43] Ikeda, S., Kishida, S., Yamamoto, H.*, et al.*: 'Axin, a negative regulator of the wnt signaling pathway, forms a complex with gsk-3 $\beta$ and $\beta$-catenin and promotes GSK-3 $\beta$-dependent phosphorylation of $\beta$-catenin', *EMBO J.*, 1998, **17**, (5), pp. 1371–1384
[44] Pecina-Šlaus, N.: 'Wnt signal transduction pathway and apoptosis: a review', *Cancer Cell Int.*, 2010, **10**, (1), p. 22
[45] Dhanasekaran, D.N., Reddy, E.P.: 'Jnk signaling in apoptosis', *Oncogene*, 2008, **27**, (48), pp. 6245–6251
[46] Szegezdi, E., Logue, S.E., Gorman, A.M.*, et al.*: 'Mediators of endoplasmic reticulum stress-induced apoptosis', *EMBO Rep.*, 2006, **7**, (9), pp. 880–885
[47] Wang, S., Binder, P., Fang, Q.*, et al.*: 'Endoplasmic reticulum stress in the heart: insights into mechanisms and drug targets', *Br. J. Pharmacol.*, 2018, **175**, (8), pp. 1293–1304
[48] Giorgi, C., Baldassari, F., Bononi, A.*, et al.*: 'Mitochondrial $Ca^{2+}$ and apoptosis', *Cell Calcium*, 2012, **52**, (1), pp. 36–43
[49] Liu, K., Shi, Y., Guo, X.*, et al.*: 'Chop mediates aspp2-induced autophagic apoptosis in hepatoma cells by releasing beclin-1 from bcl-2 and inducing nuclear translocation of bcl-2', *Cell Death Dis.*, 2014, **5**, (7), p. e1323
[50] Pinton, P., Giorgi, C., Siviero, R.*, et al.*: 'Calcium and apoptosis: er-mitochondria ca 2 + transfer in the control of apoptosis', *Oncogene*, 2008, **27**, (50), pp. 6407–6418
[51] Guo, J., Lao, Y., Chang, D.: 'Calcium and apoptosis', in Katsuhiko, M. (Ed.): '*Handbook of neurochemistry and molecular neurobiology*' (Springer, New York, 2009), pp. 597–622
[52] Mathiasen, I.S., Sergeev, I.N., Bastholm, L.*, et al.*: 'Calcium and calpain as key mediators of apoptosis-like death induced by vitamin d compounds in breast cancer cells', *J. Biol. Chem.*, 2002, **277**, (34), pp. 30738–30745